

A combination of sugar esters and chitosan to promote *in vivo* wound care

Mattia Tiboni^{1#}, Enas Elmowafy^{2#}, Marwa O. El-Derany³, Serena Benedetti¹, Raffaella Campana¹, Michele Verboni¹, Lucia Potenza¹, Francesco Palma¹, Barbara Citterio¹, Maurizio Sisti¹, Andrea Duranti¹, Simone Lucarini¹, Mahmoud E. Soliman^{2,4*}, and Luca Casettari^{1*}

¹Department of Biomolecular Sciences, University of Urbino Carlo Bo, Piazza del Rinascimento, 6, 61029 Urbino (PU), Italy.

²Department of Pharmaceutics and Industrial Pharmacy, Faculty of Pharmacy, Ain Shams University, Monazzamet Elwehda Elafrikeya Street, Abbaseyya, Cairo, Egypt, 11566

³Department of Biochemistry, Faculty of Pharmacy, Ain Shams University, Monazzamet Elwehda Elafrikeya Street, Abbaseyya, Cairo, Egypt, 11566

⁴Egypt-Japan University of Science and Technology (EJUST), New Borg El Arab, Alexandria, Egypt, 21934

*Correspondence: luca.casettari@uniurb.it; Tel. (Italy): +390722303332

ABSTRACT

In recent years, researchers are exploring innovative green materials fabricated from renewable natural substances to meet formulation needs. Among them, biopolymers like chitosans and biosurfactants such as sugar fatty acid esters are of potential interest due to their biocompatibility, biodegradability, functionality, and cost-effectiveness. Both classes of biocompounds possess the ability to be efficiently employed in wound dressing to help physiological wound healing, which is a bioprocess involving uncontrolled oxidative damage and inflammation, with an associated high risk of infection.

In this work, we synthesized two different sugar esters (*i.e.*, lactose linoleate and lactose linolenate) that, in combination with chitosan and sucrose laurate, were evaluated *in vitro* for their cytocompatibility, anti-inflammatory, antioxidant, and antibacterial activities and *in vivo* as wound care agents. Emphasis on Wnt/ β -catenin associated machineries was also set. The newly designed lactose esters, sucrose ester, and chitosan possessed sole biological attributes, entailing considerable benefit for convenient formulation of wound care products. In particular, the mixture composed of sucrose laurate (200 μ M), lactose linoleate (100 μ M), and chitosan (1%) assured its superiority in terms of efficient wound healing prospects *in vivo* together with the restoring of the Wnt/ β -catenin signaling pathway, compared with the marketed wound healing product (Healosal[®]), and single components as well. This innovative combination of biomaterials applied as wound dressing could effectively break new ground in skin wound care.

Keywords:

Antimicrobial; Antioxidant; Anti-inflammatory; Wound dressing; Wnt/ β -catenin signaling

39 1. INTRODUCTION

40 In recent years, the research of new materials is evolving to different technologies for the
41 introduction and approval of fit-for-purpose ones that can fulfill the unique requirements of novel
42 pharmaceutical and biomedical platforms in use and under development (Guth et al., 2013). From
43 an environmental impact perspective, formulation scientists have strived to explore customized
44 biomaterials, fabricated from renewable natural substances (Lukic et al., 2016; Manzoor et al.,
45 2020).

46 In this scenario, the development and characterization of new biosurfactants are becoming
47 increasingly appealing. Sugar fatty acid esters are one such class of commodities with striking
48 performance that are securing a considerable share in various industrial segments (Neta et al., 2015;
49 Pérez et al., 2017). The preponderance of these compounds over their chemical counterparts has
50 been evidenced concerning biodegradability, biocompatibility, quality, functionality, and cost-
51 effectiveness (Lucarini et al., 2016; Lukic et al., 2016). Various fatty acid and saccharide moieties
52 were conjugated to form sugar derivatives with high product output and diversity (Neta et al., 2015;
53 Zheng et al., 2015). Their surface activity and emulsifying adequacy have been well-related to the
54 sugar core and esterified fatty acid types, the number of fatty acids, and esterification degree
55 (Gumel et al., 2011; Neta et al., 2012; Teng et al., 2020; Wagh et al., 2012).

56 It is well posited that these non-ionic surfactants have best exemplified solubilizing agents,
57 permeation enhancers (PEs), stabilizing agents for biologics, as well as integral parts of various
58 delivery platforms (Elmowafy et al., 2020; Kale and Akamanchi, 2016; Klang et al., 2013; Lucarini
59 et al., 2018; McCartney et al., 2021; Schiefelbein et al., 2010; Szuts et al., 2011). In the aspect of
60 biological relevance, sugar esters have been utilized as competent therapeutic entities with biocidal
61 potentiality against pathogens including bacteria, fungi, and viruses (Matin et al., 2020; Zhang et
62 al., 2015; Zhao et al., 2015). Besides, some sugar derivatives have been recognized for their anti-
63 tumor and anti-inflammatory activities (Ferrer et al., 2005; Guan et al., 2019; Marathe et al., 2020).
64 However, the examination of their linked toxicity, at cellular and tissue levels, and cogent *in vivo*
65 studies are still limited and need to be put forward.

66 Wound healing is a complicated well-tuned bioprocess that involves sequential interlinked
67 hemostasis, inflammation, re-epithelialization, and tissue maturation, critically influencing both
68 patients and healthcare providence (Aldalaen et al., 2020; Tiboni et al., 2021). Excessive and
69 uncontrolled oxidative damage and the subsequent pathological out-of-control inflammation are the
70 underlying causes accountable for postponed and uncoordinated wound healing (Sanchez et al.,
71 2018). Functionalized wound dressings, therefore, should entail adjustable features to actively
72 participate in structural and functional skin reconstruction. Among these, wound dressings based on

73 chitosan have been extensively utilized featuring biodegradability, long-term stability, and
74 beneficial multimodal activities for wound management (*i.e.*, hemostatic, anti-inflammatory,
75 antimicrobial, antioxidant, and skin regeneration) (Feng et al., 2021; Khan and Mujahid, 2019;
76 Matica et al., 2019; Mohan et al., 2020; Saberian et al., 2021). In clinical translation scope,
77 chitosan-based wound sprays, gels, patches, bandages, and fibres are introduced on the market as
78 safe and easily applied biopolymer wound dressings (Matica et al., 2019).

79 In principle, it has been plausible to hypothesize that these biomaterials could break new ground in
80 skin wound care. Accordingly, sugar esters based on lactose with two fatty acids [*i.e.*, linoleic and
81 linolenic acids, namely lactose linoleate (C18:2 ω) and lactose linolenate (C18:3 ω), respectively]
82 were synthesized, and their aptness for mitigating skin lesions and infections was elucidated.
83 Further, their potential was compared and associated with the commercially available sucrose
84 laurate (C12), and with chitosan. To evaluate the potential impact of the present study in a
85 therapeutic application, we explored *in vitro* antioxidant, anti-inflammatory, and antimicrobial
86 properties followed by an *in vivo* wounding model study. Dermal matrices with binary and triple
87 combinations of these sugar esters and chitosan have been designed and probed as well. Healosol[®],
88 a marketed spray product containing phenytoin, was used for comparative purposes. In fact, when
89 topically applied, phenytoin was well-reported to promote wound healing via prompting fibroblast
90 proliferation and collagen deposition and possessing antibacterial efficacy (Anstead et al., 1996;
91 Shaw et al., 2007).

92 In support of our hypothesis, the underlying mechanistic impact of the utilized biomaterials on
93 wound healing was assessed *via* profiling the expression of the genes of Wnt/ β -catenin signaling
94 pathway using reverse transcription-quantitative real-time polymerase chain reaction (RT-qPCR).
95 Supporting evidences have confirmed the vital role played by the Wnt/ β -catenin signaling pathway
96 in wound healing at the molecular level (Amini-Nik et al., 2014; Yang et al., 2017; Zhang et al.,
97 2018). Indeed, canonical Wnt signaling via β -catenin and its target c-myc are critically involved in
98 cell migration, invasion, proliferation, and inflammatory events during the wound healing process
99 (Lamouille et al., 2014). Interestingly, recent reports showed that natural compounds including
100 chitosan might modulate Wnt/ β -catenin signaling in various diseases (Hu et al., 2018; Sferrazza et
101 al., 2020). To the best of the authors' knowledge, no data on the functional contributes of these
102 innovative wound healing frontiers are available. Additionally, the effect of sugar esters and
103 chitosan on the stringent control of the molecular expressions of key factors in Wnt/ β -catenin
104 signaling that affects wound healing is far from clear.

105

106 2. MATERIALS AND METHODS

107 2.1 Materials

108 Chitosan chloride (Chitoceuticals[®] Chitosan HCl code 54040) was purchased from Heppe Medical
109 Chitosan GmbH (Halle, Germany), linolenic and linoleic acids from Fluorochem (Hadfield, UK),
110 triethylamine (Et₃N) anhydrous from TCI (Zwijndrecht, Belgium), lactose monohydrate and 4-
111 (dimethylamino)pyridine (DMAP) from Carlo Erba (Milan, Italy). Sucrose monolaurate, *p*-
112 toluenesulfonic acid, 2,2-dimethoxypropane, 1-(3-dimethylaminopropyl)-3-ethylcarbodiimide
113 hydrochloride (EDCI·HCl), tetrafluoroboric acid diethyl ether complex (HBF₄·Et₂O), carbonyl
114 cyanide 4-(trifluoromethoxy) phenylhydrazone (FCCP), and all organic solvents used were
115 purchased from Sigma-Aldrich (Milan, Italy). Healosol[®] spray (phenytoin) was obtained from the
116 Egyptian company for advanced pharmaceuticals (Egypt). Prior to use dichloromethane (CH₂Cl₂)
117 was dried with molecular sieves with an effective pore diameter of 4 Å. The structure of compounds
118 was unambiguously assessed by MS, ¹H NMR, and ¹³C NMR. ESI-MS spectra were recorded with
119 a Waters Micromass ZQ spectrometer in a negative or positive mode using nebulizing nitrogen gas
120 at 400 L/min and a temperature of 250 °C, cone flow 40 mL/min, capillary 3.5 kV, and cone
121 voltage 60 V; only molecular ions [M-H]⁻, [M+NH₄]⁺ or [M+Na]⁺ are given. ¹H NMR and ¹³C
122 NMR spectra were recorded on a Bruker AC 400 or 101, respectively, spectrometer and analyzed
123 using the TopSpin 1.3 software package. Chemical shifts were measured by using the central peak
124 of the solvent. Column chromatography purifications were performed under “flash” conditions
125 using Merck 230–400 mesh silica gel. TLC was carried out on Merck silica gel 60 F254 plates,
126 which were visualized by exposure to ultraviolet light and to an aqueous solution of ceric
127 ammonium molybdate.

128

129 2.2 Methods

130 2.2.1 Synthesis of lactose-based surfactants

131 2.2.1.1 General procedure for the synthesis of lactose tetra acetate monoesters 6'-*O*-octadec-9*Z*-
132 12*Z*-dienoyl- and 6'-*O*-octadec-9*Z*-12*Z*-15*Z*-trienoyl-4-*O*-(3',4'-*O*-isopropylidene-β-D-
133 galactopyranosyl)-2,3:5,6-di-*O*-isopropylidene-1,1-di-*O*-methyl-D-glucopyranose (**3a,b** – Scheme
134 1).

135 DMAP (0.048 g, 0.4 mmol) and linoleic acid (**1a**) or linolenic acid (**1b**) (2 mmol) were added to a
136 solution of 4-*O*-(3',4'-*O*-isopropylidene-β-D-galactopyranosyl)-2,3:5,6-di-*O*-isopropylidene-1,1-di-
137 *O*-methyl-D-glucopyranose (lactose tetra acetate, LTA) (**2**) (1.22 g, 2.4 mmol) in dry CH₂Cl₂ (20.0
138 mL) at room temperature under N₂ atmosphere. The mixture was cooled at 0 °C and added of Et₃N
139 (2.4 mmol, 0.334 mL) and EDCI·HCl (0.460 g, 2.4 mmol), then stirred at 0 °C for 10 minutes and at

140 room temperature for 3 days, diluted with CH₂Cl₂, and washed with saturated aqueous NH₄Cl and
141 NaHCO₃ solutions. The organic phase was dried on Na₂SO₄, filtered, and concentrated. Purification
142 of the residue by column chromatography (cyclohexane/EtOAc 7:3) gave **3a,b** as a pale yellow oil.

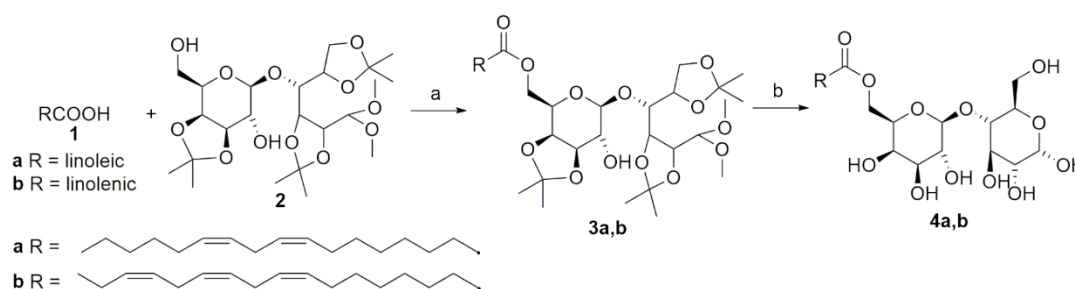
143

144 2.2.1.2 General procedure for the synthesis of lactose fatty acid monoesters 6'-*O*-octadec-9*Z*-12*Z*-
145 dienoyl- and 6'-*O*-octadec-9*Z*-12*Z*-15*Z*-trienoyl-4-*O*-(β-D-galactopyranosyl)-D-glucopyranose
146 (**4a,b**).

147 Compounds **3a** or **3b** (0.38 mmol) were dissolved in H₂O (0.030 mL) and CH₃CN (3 mL),
148 HBF₄·Et₂O (0.006 mL) was added and the mixture was stirred at 0 °C for 5 h. The white solid
149 precipitated was filtered, washed with CH₃CN and dried. Trituration with petroleum ether gave **4a,b**
150 as white solids.

151 Yields, ESI-MS, and NMR characterizations are reported in the supplementary material.

152



154 **Scheme 1.** Reagents and conditions: (a) EDCI·HCl, DMAP, dry TEA, dry CH₂Cl₂, 0 °C 10' then r.t. 72 h; (b)
155 HBF₄·Et₂O, H₂O, CH₃CN, 0 °C, 5 h.

156

157 2.2.2 Cell culture

158 HaCaT (immortalized human keratinocytes) and RAW 264.7 (murine macrophages) cell lines were
159 used to investigate the biological properties of chitosan and sugar-based esters. Cells were grown in
160 Dulbecco's modified eagle's medium (DMEM) medium supplemented with 10% fetal bovine
161 serum, 1% L-glutamine, and 1% penicillin/streptomycin 100 U/mL, and maintained in a CO₂
162 incubator at 37 °C and 5% CO₂. Cell culture reagents were from Sigma-Aldrich (Milan, Italy).

163

164 2.2.3 Cell viability assays

165 HaCaT cell viability after chitosan and sugar-based ester administration was analyzed by water-
166 soluble tetrazolium (WST)-8 and sulphorodamine B (SRB) assays, which evaluate cell metabolic
167 activity and cell protein content, respectively. Briefly, cells (5x10³/well) were seeded in 96-well
168 plates and treated for 2 h with chitosan (0.01-1%) or sugar-based esters (6.25-200 μM). Test
169 compounds were then removed and fresh medium added. After 24 h of incubation, WST-8 (Sigma-

170 Aldrich, Milan, Italy) was added to each well, and cells were further incubated at 37 °C up to 4 h
171 (Catalani et al., 2017b). Color development was monitored at 450 nm in a multiwell plate reader
172 (BioRad Laboratories, Hercules, USA). In the same 96-well plate, the SRB test was then performed,
173 as previously published (Farabegoli et al., 2017). Briefly, cell culture medium was removed, cells
174 fixed with 50% trichloroacetic acid for 1 h at 4 °C, rinsed with water, and incubated for 30 min with
175 0.4% SRB solution (Sigma-Aldrich, Milan, Italy). After rinsing with 1% acetic acid and
176 solubilizing in 10 mM Tris for 10 min, absorbance was measured at 570 nm in a microplate reader
177 (BioRad Laboratories, Hercules, USA). Data were expressed as cell growth (%) versus non-treated
178 cells (controls).

179

180 **2.2.4 Nitric oxide detection**

181 The anti-inflammatory properties of chitosan and sugar-based esters were evaluated in RAW 264.7
182 cells stimulated by lipopolysaccharide (LPS, Sigma-Aldrich, Milan, Italy). Briefly, cells
183 (3×10^4 /well) were seeded in 96-well plates and treated for 2 h with chitosan (0.01-0.5%) or sugar-
184 based esters (25-50 μ M). Test compounds were then removed and cells stimulated with 1 μ g/mL
185 LPS for 24 h. After incubation, nitric oxide (NO) levels were determined in the medium by mixing
186 equal volumes of supernatant and Griess reagent (Sigma-Aldrich, Milan, Italy) (Bryan and
187 Grisham, 2007). Absorbance was measured at 570 nm using a plate reader (BioRad Laboratories,
188 Hercules, USA). In the same 96-well plate, an SRB test was also performed as described above, to
189 evaluate RAW 264.7 cell viability after LPS treatment.

190

191 **2.2.5 Evaluation of antioxidant properties (DPPH and DCFH-DA assays)**

192 The ability of chitosan and sugar-based esters to act as antioxidants was evaluated by the 2,2-
193 diphenyl-1-picryl-hydrazyl-hydrate (DPPH) radical scavenging assay, as previously described
194 (Saltarelli et al., 2019). Chitosan was solubilized and diluted in water (tested concentrations 0.01-
195 1%), while sugar-based esters were first dissolved in dimethyl sulfoxide (DMSO) and then diluted
196 in ethanol (EtOH) (tested concentrations 6.25-200 μ M). DPPH (100 μ M, Sigma-Aldrich, Milan,
197 Italy) was prepared in EtOH. The scavenger effect was expressed as $\% = [(\text{OD } 517 \text{ nm control} - \text{OD}$
198 $517 \text{ nm sample} / \text{OD } 517 \text{ nm control}] \times 100$. EC_{50} values (*i.e.*, the concentration required to obtain a
199 50% antioxidant effect) werethen calculated.

200 Moreover, the antioxidant properties of chitosan and sugar-based ester were analyzed in HaCaT
201 cells by 2',7'-dichlorofluorescein diacetate (DCFH-DA, Sigma-Aldrich, Milan, Italy), which turns to
202 highly fluorescent 2',7'-dichlorofluorescein (DCF) upon oxidation (Catalani et al., 2017a). Briefly,
203 cells (1×10^4 /well) were seeded in black 96-well plates and incubated for 2 h with chitosan (0.01-

204 1%) or sugar-based esters (100 μM). Test compounds were then removed and DCFH-DA (5 μM)
205 added to each well for 30 min at 37 °C. After excess probe removal, cells were treated with
206 hydrogen peroxide (H_2O_2 , 100 μM) for 30 min and DCF fluorescence emission measured at ex/em
207 485/520 nm in the multiwell plate reader FluoStar Optima (BMG Labtech, Germany). Data were
208 expressed as relative oxidation versus non-oxidized cells.

209

210 **2.2.6 DNA nicking assay**

211 The protective effect of chitosan and sugar-based esters against DNA oxidative damage was
212 evaluated by the DNA nicking assay, which employs ferrous ions and dioxygen ($\text{Fe}^{2+} + \text{O}_2$) to
213 generate free radical-induced DNA strand breaks. A cell-free system composed of supercoiled
214 pEMBL8 plasmid DNA, which resembles the structure of mtDNA, was used (Mari et al., 2018).
215 Briefly, plasmid DNA (5.8 $\mu\text{g}/\text{mL}$) was incubated in PBS in the presence of different amounts of
216 sugar-based surfactants (from 1.2 mM to 40 μM) or chitosan (from 0.5% to 0.02% w/v) in a volume
217 of 72 μL . DNA damage was generated by adding 8 μl of freshly made 3 mM ferrous sulphate (final
218 $\text{Fe}^{2+} = 300 \mu\text{M}$), and after 10 minutes, the reaction was stopped by adding 40 μL of Orange G
219 loading buffer. The disappearance of the supercoiled form of the plasmid was assessed on an
220 ethidium bromide-stained agarose gel electrophoresis followed by the quantitation by Gel Doc 2000
221 and Quantity One software (Bio-Rad). The EC_{50} values were calculated determining the
222 concentration of the compound that protects half of the supercoiled plasmid.

223

224 **2.2.7 Microorganisms culture conditions**

225 In this study, several strains of human clinical isolates of *Staphylococcus aureus* [*S. aureus*
226 HCS026, *S. aureus* 2/5, *S. aureus* 28/10, *S. aureus* 18/9, *S. aureus* HCS002 methicillin-resistant
227 (MRSA)], as well as the clinical isolate *Pseudomonas aeruginosa* C86, belonging to the strain
228 collection of Pharmacology and Hygiene Division (Department of Biomolecular Sciences,
229 University of Urbino), were used. The reference strains, *S. aureus* ATCC 43387, *S. aureus* ATCC
230 43300 and *P. aeruginosa* ATCC 27583 were also included. All the *S. aureus* strains were cultured
231 in Tryptone soy agar (TSA) (VWR, Milan, Italy) and subcultured in Mannitol Salt Agar (MSA)
232 (VWR) at 37°C for 24 h, while *Pseudomonas* strains were grown in Cetrimide agar (VWR) at the
233 same culture conditions; all the strains were stored at -80 °C in Nutrient broth (VWR)
234 supplemented with 20% glycerol.

235 Pathogenic filamentous dermatophytes belonging to the strain collection of Pharmacology and
236 Hygiene Division (Department of Biomolecular Sciences, University of Urbino) (*Trichophyton*
237 *mentagrophytes* F6, *Trichophyton rubrum* F2, *Trichophyton violaceum* F11, *Epidermophyton*

238 *floccosum* F12) and the reference strain *Candida albicans* ATCC 10231 were also included. The
239 dermatophytes were maintained on Potato Dextrose Agar (PDA) (VWR) at 35°C for 7 days, while
240 *C. albicans* at 37 °C for 24 h.

241

242 **2.2.8 Minimum inhibitory concentration and checkboard**

243 For each molecule, the minimum inhibitory concentration (MIC) was determined following the
244 standard microdilution method (Clinical and Laboratory Standards Institute CLSI, 2017). For
245 filamentous fungi and mycete the conidial suspensions were prepared according to the CLSI M38-A
246 and CLSI M27-A protocol respectively.

247 At first, each compound was dissolved (5 mg/mL) in DMSO of biological grade (Sigma, Milan,
248 Italy) to obtain concentrated stock solutions. In the case of sucrose laurate, the stock solution was
249 prepared in distilled water and then 0.22 µm filtered. Preliminary assays were performed to exclude
250 the possible bacteriostatic and/or bactericidal activity of the solvent; in any case, the volume of
251 DMSO never exceeded 5% (v/v) of the final total volume. Chitosan was dissolved in water with 1%
252 acetic acid to a final concentration of 4% (w/v) and left overnight at 70 °C with gentle stirring.
253 Afterward, the solution was autoclaved at 121 °C for 15 min and then maintained at room
254 temperature until use.

255 One colony of each bacterial strain was inoculated in 10 mL of Tryptone Soy Broth (TSB) (VWR)
256 and incubated at 37 °C for 18 h. The bacterial suspensions were adjusted to about 10⁶ CFU/mL (OD
257 _{610nm} 0.13-0.15) in Mueller Hinton Broth II (MHB II) (VWR) and 100 µL was added to wells of the
258 96-well plate together with the appropriate volumes of each sugar-based monoester solution (from
259 2048 to 16 µg/mL). In the case of chitosan, the used concentrations ranged from 2% to 0.25%. Two
260 rows were used as positive and negative controls inoculating bacteria alone and MHB II alone
261 respectively. MIC was defined as the lowest concentration of compound able to inhibit bacterial
262 growth after 24 h of incubation at 37 °C. All data were expressed as the mean of three independent
263 experiments performed in duplicate.

264 As regards the filamentous fungi, spores were harvested from PDA plate by adding 2 mL of sterile
265 0.85% saline solution supplemented with 0.05% Tween 80; the surface was scraped with a sterile
266 cotton swab, and the suspension was transferred in a sterile tube and left at room temperature for 5
267 min to allow the sedimentation of hyphal fragments. Afterward, the homogeneous upper suspension
268 was vortexed for 15 s and adjusted to an optical density (OD 530 nm) between 0.09 and 0.4
269 corresponding to about 10⁶ spores/mL. For *C. albicans* the mixture suspension was adjusted with a
270 spectrophotometer to a turbidity of 0.12 (about 10⁷ cfu/mL). Successively, 100 µL of each fungal
271 suspension was diluted 1:50 in standard RPMI 1640 medium (Sigma) and inoculated into 96-well

272 plates together with the appropriate volumes of each test solution as described above. Two rows
273 were left for positive control growth and negative controls (medium only), respectively.
274 Undecylenic acid was used as internal control molecule. Plates were incubated at 35 °C for
275 dermatophytes and 37 °C for 48 h for *C. albicans* and examined after 48 h of incubation. MIC is
276 defined as the lowest drug concentration that inhibits visible growth in comparison with the control
277 (untreated sample). In addition, the turbidity of the 96-wells plate was assessed by
278 spectrophotometer (530 nm) (Multiskan EX, Thermo Scientific, Italy).

279 The synergy of the most active sugar-based monoester (sucrose laurate) and chitosan against
280 representative bacterial strains chosen based on their MIC values (*S. aureus* 2/5, *S. aureus* 18/19
281 and *P. aeruginosa* C86) was evaluated by the checkerboard method. The interactions between the
282 combinations of sucrose laurate and chitosan were indicated by the fractional inhibitory
283 concentration (FIC) index for each compound. The former was performed using 2-fold increasing
284 concentrations of each compound (from the related MIC values up to 8 µg/mL) and chitosan (from
285 1% to 0.25% v/v). In the case of the compounds dissolved in DMSO, the upper limit of the
286 concentrations range tested was determined considering a final concentration of 1% DMSO. The
287 value of FIC index was interpreted as follows: ≤ 0.5, synergy; > 0.5 and ≤ 1.0, additive; > 1.0 and <
288 4, indifferent; ≥ 4, antagonistic.

289

290 **2.2.9 Haemolysis Assays**

291 The haemolysis of compounds was evaluated as described by Chongsiriwatana et al.
292 (Chongsiriwatana et al., 2008). Briefly, 4 mL of freshly drawn, heparinized human blood was
293 diluted with 25 mL of phosphate buffered saline (PBS), pH 7.4. After washing three times in 25 mL
294 of PBS, the pellet was resuspended in PBS to ~20 vol %. A 100 µL amount of erythrocyte
295 suspension was added to 100 µL of different concentrations of the most active sugar-based
296 monoesters and chitosan respectively (starting from the related MIC values). PBS and 0.2 % Triton
297 X-100 were used as negative and positive control, respectively. Each condition was tested in
298 triplicate. After 1 h of incubation at 37 °C each well was centrifuged at 1200 G for 15 min, the
299 supernatant was diluted 1:3 in PBS and transferred to a new plate. The OD₃₅₀ was determined using
300 the Synergy HT microplate reader spectrophotometer (BioTek, Winooski, VT, USA).

301 The haemolysis (%) was determined as reported in Eq. 1:

302

$$303 \quad [(A - A_0)/(A_{\text{total}} - A_0)] \times 100 \quad (1)$$

304

305 where A is the absorbance of the test well, A_0 the absorbance of the negative control, and A_{total} the
306 absorbance of the positive control; the mean value of three replicates was recorded.

307

308 **2.2.10 Stability to serum protease**

309 The sugar-based monoesters and the chitosan were pre-incubated in fresh 50% blood plasma
310 solution for 0, 3, and 6 hours at 37 °C (Chongsiriwatana et al., 2008). Briefly, a representative
311 bacterial strain (*i.e.*, *S. aureus* ATCC 43300) was grown for 6 h in BH broth and diluted in Mueller
312 Hinton II (Oxoid, Milano, Italy) to give a final concentration of 1.5×10^6 CFU/mL. Fresh human
313 blood cells were centrifuged at 3000 rpm for 5' to separate the plasma from the red blood cells. For
314 the selected sugar-based monoesters three aliquots were dissolved in DMSO at a concentration of
315 2048 µg/mL and diluted 2-fold in the plasma to reach the final concentration of 1024 µg/mL. In the
316 case of chitosan, it was 2-fold diluted in the plasma to reach the final concentration of 1%. The
317 samples were incubated at 37 °C for 0, 3, and 6 h and then used to perform MIC assays according to
318 the broth microdilution method in 96-well microtiter plates, as mentioned above. No difference of
319 MIC values among the trials performed in different plasma-preincubation times attests the plasma
320 stability.

321

322 **2.2.11 *In vivo* wound healing model**

323 2.2.11.1 Animals used

324 Seventy-two male Wistar albino rats weighing 150-180 g were used for *in vivo* study. The rats were
325 provided with a standard normal diet and drinking water during the experiment. Rats were caged in
326 open cages at 25 °C with 12 h light and dark cycles at the animal facility of the Faculty of
327 Pharmacy (Ain Shams University, Egypt) and were left for one week for acclimatization before
328 starting the experiment. All animal experimental work was approved by the Ethics Committee at the
329 Faculty of Pharmacy, Ain shams university, Egypt, and conducted according to the U.K. Animals
330 (Scientific Procedures) Act, 1986 and the EU Directive 2010/63/EU guidelines for animal studies.

331

332 2.2.11.2 Wound excision model

333 Wounds were induced on the sterilized shaved dorsal skin of rats after being anesthetized using
334 intraperitoneal (IP) ketamine (50 mg/kg). One circular excision wound was induced with blunt
335 dissection (20 mm in diameter) and the wound was left exposed.

336

337

338

339 2.2.11.3 Experimental design

340 The experimental model duration was fifteen days. The study included twelve equal groups of rats,
341 each group consisting of six rats. The appraisal of delivery potential of chitosan, sucrose laurate,
342 lactose linoleate, and lactose linolenate, either alone or their dual and triple combinations was
343 explored on wound healing. The therapeutic effect of the proposed wound care products was
344 compared with that of the marketed wound healing product (Healosol[®]). The twelve experimental
345 groups were coded as reported in supplementary material Table 1. The wounds were induced on the
346 upper side of the dorsal skin received the treatment, while the control group was unwounded rats.
347 The formulations under investigation were topically applied on the formed wounds daily for 15
348 days at the concentrations reported in supplementary material Table 1. For each group, photography
349 of wounds was performed using a digital camera on days 3.5, 7, and 15. The wound condition and
350 percentage of wound healing were recorded via measuring the diameter of the wound in mm.
351 Two weeks after wound induction, rats were sacrificed by cervical dislocation; skin tissues were
352 excised at the wound areas and washed with ice-cold saline. Afterward, parts of tissues were stored
353 at -80 °C until RNA extraction for assessment of gene expression, while the other parts were
354 immediately immersed in appropriate buffer for histological examination and staining.

355

356 **2.2.12 Histopathological assessment and collagen quantification**

357 Rats were euthanized and the formed granulation tissue was excised leaving a 5 mm margin of
358 normal skin. Skin samples were flushed and fixed in 10% neutral buffered formalin for 72 h.
359 Samples were trimmed and processed in serial grades of ethanol, cleared in xylene, samples were
360 infiltrated and embedded into Paraplast tissue embedding media. 4 µm thick tissue sections were cut
361 by rotatory microtome for demonstration of skin layers in different samples.

362 Tissue sections were stained by Hematoxylin and Eosin (H&E) as a general morphological
363 examination staining method and examined by using a light microscope (Leica Microsystems
364 GmbH, Wetzlar, Germany) and lesions were recorded. Microscopic examination lesion score
365 system was adopted blind to the treatment conditions as previously described (Al-Sayed et al.,
366 2020).

367 Furthermore, tissue sections from all groups were stained by Trichrome stain kit to stain
368 collagenous connective tissue fibers, then examined by using a light microscope (Leica
369 Microsystems GmbH, Wetzlar, Germany). Six non-overlapping fields were randomly selected and
370 scanned from dermal layers of each sample for the determination of area percentage of reactive
371 collagen fibers to Masson's trichrome stain in six tissue samples. All light microscopic examination

372 and data were obtained by using the Leica Application module for histological analysis attached to
373 Full HD microscopic imaging system (Leica Microsystems GmbH, Germany).

374

375 **2.2.13 Reverse transcription-quantitative real-time polymerase chain reaction(RT-qPCR)**

376 Determination of gene expression of Wnt/ β -catenin signaling pathway involved in wound healing
377 was done using RT-qPCR. The expression of wingless-type MMTV integration site family1
378 (Wnt1), Wnt 2, c-myc, and beta-catenin (β -catenin) genes were measured and normalized to β -actin
379 gene as reference gene. Sequences of PCR primer sets used are shown in supplementary material
380 Table 2.

381 Total RNA was extracted from the wound tissue using Trizol (Thermo Scientific co., USA).
382 Subsequently, RNA was reversely transcribed using a high-capacity cDNA Synthesis Kit (Thermo
383 Scientific co., USA). RT-qPCR was performed using an ABI 7500 RT-PCR System (Applied
384 Biosystems, Foster City, CA, USA). The relative quantification was then calculated by the $2^{-\Delta\Delta Ct}$
385 method.

386

387 **2.2.14 Statistical analysis**

388 Comparisons between multiple means were performed via ANOVA followed by post hoc analysis
389 for significance (Tukey test). The level of significance was set at $p < 0.05$. Statistics were performed
390 using GraphPad Prism 6.0 (GraphPad Software, Inc., San Diego, CA, USA).

391 **3. RESULTS AND DISCUSSION**

392 **3.1 Lactose esters synthesis and chitosan characterization**

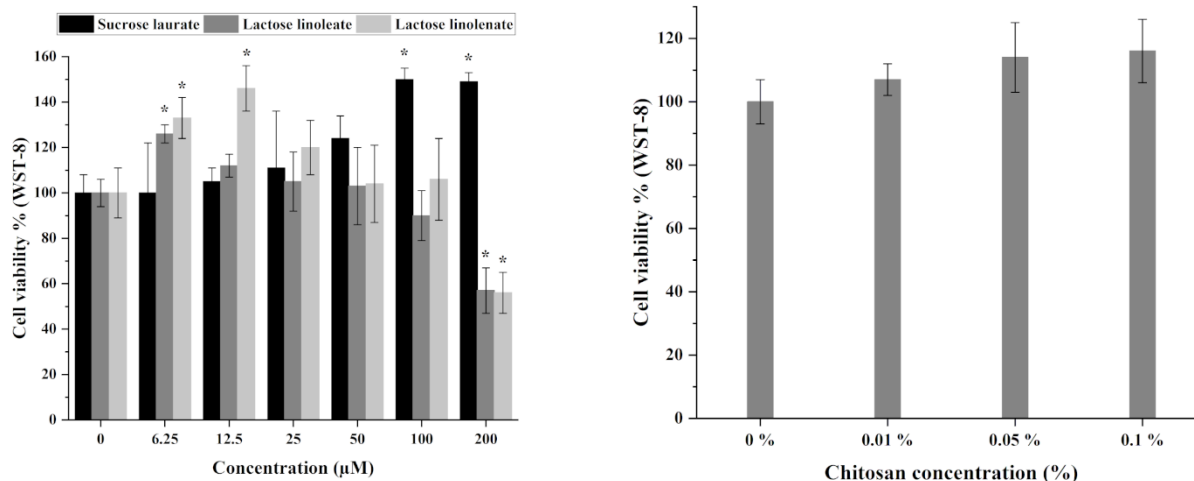
393 The synthesis of lactose linoleate (**4a**) and lactose linolenate (**4b**) was conducted as described in
394 scheme 1. For the coupling reaction of the acids (**1**) with LTA (**2**) (Hough et al., 1979) a modified
395 Steglich esterification (Neises and Steglich, 1978) (EDCI coupling as agent instead of DCC) was
396 found to be the most effective procedure to obtain the products **3a,b** in pure form. In fact, by using
397 the Lypozyme[®] approach, which requires a high temperature (75 °C) for a relative long time (12 h)
398 (Perinelli et al., 2018) or the activation of the acid as acyl chloride (Campana et al., 2019), which
399 utilizes aggressive thionyl or oxalyl chlorides, several isomerizations of the double bonds in the
400 corresponding linoleate and linolenate esters **3a,b** were observed. Finally, a classical deprotection of
401 LTA-esters **3a,b** was carried out by using catalytic HBF₄·Et₂O (McCartney et al., 2021) to obtain the
402 desired free sugar esters **4a,b** in good yield.

403 Chitosan HCl was characterized using a GPC-SE chromatography reporting a number average (Mn)
404 of 133,285 and a weight average (Mw) of 159,310 with a polydispersity (PDI) of 1.195.

405

406 **3.2 Chitosan and sugar-based esters showed comparable *in vitro* HaCaT cell compatibility** 407 **profile**

408 HaCaT cell viability after chitosan and sugar-based ester administration was analyzed both by
409 WST-8 (Figure 1 and supplementary material Table 3) and SRB (Supplementary material Figure 1
410 and SM Table 4) assays, leading to comparable results. Referring to chitosan, no cytotoxic effects
411 were observed on cell growth with chitosan concentrations between 0.01 and 0.1%. It is worth
412 mentioning that results obtained with higher concentrations; 0.5 and 1% were excluded due to
413 interferences with the assays. As regards sugar-based esters, sucrose laurate promoted significant
414 cell growth at all tested concentrations, while lactose linoleate and lactose linolenate showed
415 suppression of cell viability, reaching < 80% cell viability only at the maximum tested dose (200
416 μM).



417
418 **Figure 1.** HaCaT cell viability after chitosan and sugar-based ester administration evaluated with WST-8 assay.
419
420

421 **3.3 Antioxidant and radical scavenging properties of chitosan and sugar-based esters by**
422 **DPPH, DCFH-DA, and DNA nicking assays**

423 The radical scavenging ability of chitosan and sugar-based esters evaluated by the DPPH assay is
424 reported in supplementary material Table 5. Chitosan 0.5 and 1% presented a weak but significant
425 scavenger effect against the DPPH radical (EC_{50} equal to $6.93 \pm 0.54\%$). Sucrose laurate did not
426 show appreciable antioxidant properties within the range of concentrations tested. This finding was
427 previously reported, where sucrose laurate was reported to negatively affect the scavenging
428 performance of some natural products (Kim et al., 2009).

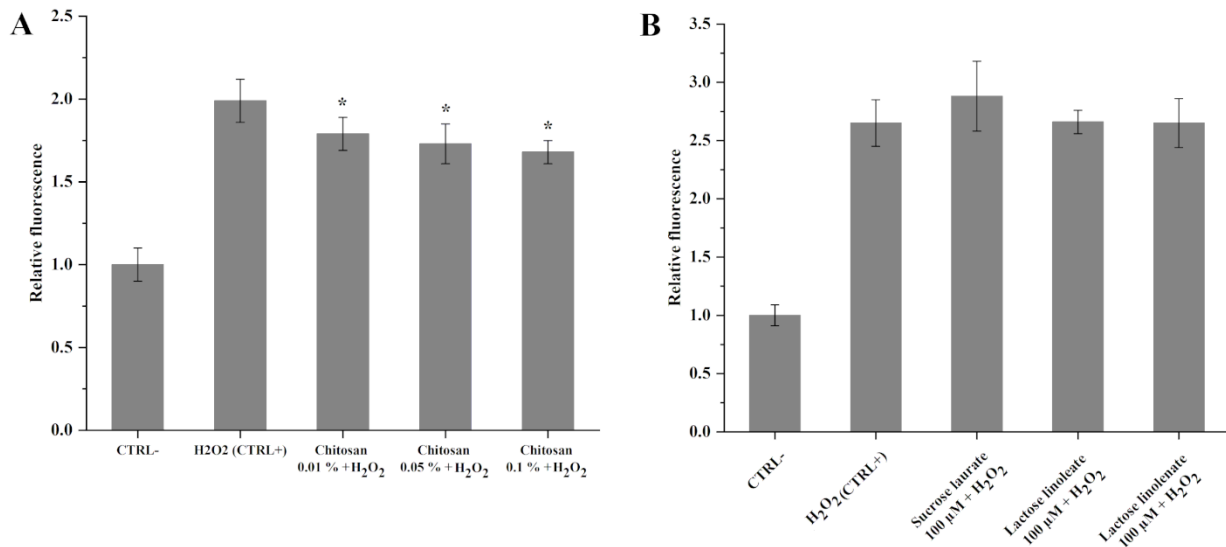
429 On the other side, lactose linoleate and lactose linolenate had EC_{50} values equal to $407 \pm 11 \mu\text{M}$ and
430 $396 \pm 8 \mu\text{M}$, respectively.

431 Regarding the DNA nicking assay, the ability of sugar based surfactants and chitosan to protect
432 plasmid DNA was evaluated quantitatively on supercoiled pEMBL8 and expressed as EC_{50} .
433 Sucrose laurate showed no protection ($EC_{50} > 3 \text{ mM}$), while lactose linoleate and lactose linolenate
434 moderately protected DNA with EC_{50} values of $0.51 \pm 0.08 \text{ mM}$ and $0.60 \pm 0.07 \text{ mM}$, respectively. At
435 the same time, the presence of chitosan interfered with DNA electrophoresis, thus we were not able
436 to determine its EC_{50} value.

437 As indicated in Figures 2A, and B, H_2O_2 administration (CTR+) to HaCaT cells led to a significant
438 increment of DCF fluorescence emission as compared to untreated cells (CTR-). When cells were
439 pre-treated for 2 hours with chitosan 0.01-0.1%, a significant reduction of H_2O_2 -induced oxidation
440 was observed (Figure 2A, * $p < 0.05$ vs. CTR+). However, results obtained with chitosan 0.5 and 1%
441 were excluded due to interferences with the assay. When cells were pre-treated for 2 hours with

442 sugar-based esters 100 μ M (Figure 2B), no appreciable decrement of H₂O₂-induced oxidation was
443 revealed.

444



445

446

Figure 2. Evaluation of the antioxidant properties of chitosan and sugar-based esters in HaCaT cells

447

448 **3.4 Chitosan and sugar-based esters manifested anti-inflammatory features in RAW 264.7** 449 **cells**

450 As reported in Figure 3, the administration of LPS to RAW 264.7 cells led to NO production and
451 release in the culture medium, while NO could not be quantified in untreated control cells. When
452 cells were pre-treated for 2 hours with chitosan 0.1 and 0.5%, a significant reduction of LPS-
453 induced NO release was observed (Figure 3A). However, the evaluation of cell viability by SRB
454 test revealed that NO reduction was due to a parallel decrement of cell growth (Supplementary
455 material Figure 2A). At non toxic concentrations (0.01 and 0.05%), chitosan did not significantly
456 reduce NO release. In fact, the anti-inflammatory properties of chitosan and NO production is
457 directly related to its molecular weight. Whereas, larger chitosans were found to significantly
458 inhibit the NO production, on the other hand smaller chitosans significantly increase NO production
459 (Chang et al., 2019).

460

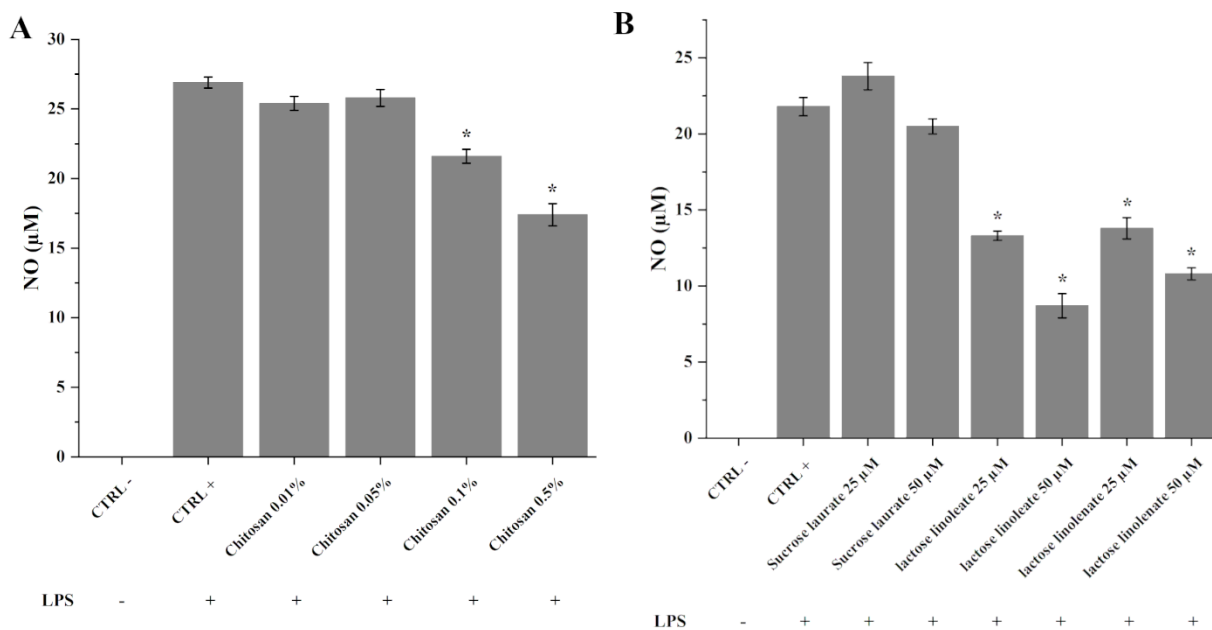


Figure 3. Evaluation of the anti-inflammatory properties of chitosan and sugar-based esters in RAW 264.7 cells. *p < 0.05 vs. CTRL +.

461
462
463
464

465 Referring to sugar-based esters, a significant reduction of LPS-induced NO release was observed in
466 RAW 264.7 cells pre-treated for 2 hours with lactose linoleate and lactose linolenate (Figure 3B).
467 However, the evaluation of cell viability by SRB test revealed that NO reduction by lactose
468 linoleate was partially due to a concomitant decrement of cell growth (Supplementary material
469 Figure 2B). Sucrose laurate did not affect NO release; therefore, at the concentrations tested, lactose
470 linolenate was the only sugar-based ester revealing anti inflammatory properties without presenting
471 cytotoxic effects.

472 The incubation of RAW 264.7 cells with chitosan (0.01-0.5%) or sugar-based esters (25-50 µM)
473 alone was not associated with NO release in the extracellular medium (data not shown).

474

475 **3.5 Evaluation of antimicrobial and antifungal effects of chitosan and sugar-based esters**

476 Data on the antibacterial activity of the examined compounds are summarized in Table 1. As
477 expected, chitosan revealed antimicrobial activity against all the tested microorganisms with MIC
478 values ranging between 1 and 2% (w/v) due to its wide range of antibacterial activities (Abd El-
479 Hack et al., 2020). As regards the sugar-based monoesters, lactose linolenate exhibited MIC values
480 of 1024 µg/mL against notmethicillin-resistant *S. aureus* strains (*S. aureus* HCS026, *S. aureus* 2/5,
481 *S. aureus* 28/10, *S. aureus* 18/9, and *S. aureus* ATCC 43387), resulting in efficacy against the
482 MRSA strains (*S. aureus* HCS002 and *S. aureus* ATCC 43300) and *P. aeruginosa* strains. Sucrose
483 laurate evidenced the greatest antimicrobial activity, reaching the lowest MIC values (256 µg/mL)
484 against *S. aureus* HCS026, *S. aureus* 28/10, *S. aureus* 18/9 and *S. aureus* ATCC 43387. This

485 finding agreed with recent reports that highlighted a potent antimicrobial activities for sucrose fatty
 486 acid esters as sucrose monolaurate due to its physical properties, which effect on the wettability of
 487 solids that inturns alters the adhesion of microorganisms to the surface (Krawczyk, 2018).
 488 The possible synergy between the most active sugar-based monoesters (sucrose laurate) and
 489 chitosan was also determined. In most cases, the obtained fractional inhibitory concentration index
 490 (FICI) indicate an "indifferent" effect of the molecules between them (FICI = 2), and only in the
 491 case of *S. aureus* 28/10 an additive effect has been observed (FICI = 0.75) (data not shown).

492

493 **Table 1.** Antimicrobial activity of chitosan and sugar-based monoesters assessed against *S. aureus* and *P. aeruginosa*
 494 strains.

	Chitosan (%)	Sucrose laurate ($\mu\text{g/mL}$)	Lactose linoleate ($\mu\text{g/mL}$)	Lactose linolenate ($\mu\text{g/mL}$)
<i>S. aureus</i> HCS026	2	256	1024	1024
<i>S. aureus</i> 2/5	1	1024	>1024	1024
<i>S. aureus</i> 28/10	1	256	>1024	1024
<i>S. aureus</i> 18/9	1	256	>1024	1024
<i>S. aureus</i> MRSA HCS002	1	1024	>1024	>1024
<i>S. aureus</i> ATCC 43300	1	1024	>1024	>1024
<i>S. aureus</i> ATCC 43387	2	256	1024	1024
<i>P. aeruginosa</i> C86	2	1024	>1024	>1024
<i>P. aeruginosa</i> ATCC 27583	1	1024	>1024	>1024

495

496 Data on antifungal activity of the examined compounds are summarized in supplementary material
 497 Table 6. Chitosan revealed to be active against all the tested microorganisms with MICs ranging
 498 between 1 and 2% (w/v), while sugar-based surfactants (e.g. lactose linolenate and sucrose laurate)
 499 showed antifungal activity with MIC between 128 $\mu\text{g/mL}$ and 256 $\mu\text{g/mL}$ in the case of *T.*
 500 *mentagrophytes* F6, *E. floccosum* F12 and *C. albicans*, higher than 521 $\mu\text{g/mL}$ for the other strains.
 501 Among the tested molecules, sucrose monolaurate showed the greatest antifungal activity with
 502 MICs ranging from 128 $\mu\text{g/mL}$ to 256 $\mu\text{g/mL}$.

503

504 **3.6 Evaluation of chitosan and sugar-based esters *in vitro* blood compatibility profile and**
505 **stability in plasma**

506 The toxicity of these compounds toward mammalian cells was assessed determining their ability to
507 lyse human erythrocytes (Supplementary material Table 7). As shown, chitosan (from 1 to 0.25%)
508 showed very low haemolytic activity with values ranging from 2.97% to 1.53%; similarly, lactose
509 linolenate resulted to be not toxic with haemolytic activity of 5.6% at its MIC value (1024 µg/mL),
510 up to haemolytic activity of 0.73% at lower concentration. On the contrary, sucrose laurate was able
511 to lyse human erythrocytes up to a concentration of 256 µg/mL (haemolytic activity 12.09%),
512 exhibiting low extent of haemolytic activity (1.8%) at lower concentration (128 µg/mL).

513 As regards the stability to serum proteases (Supplementary material Table 8), the MIC of chitosan,
514 sucrose laurate, and lactose linolenate against *S. aureus* ATCC 43300 in 50% blood plasma,
515 resulted unvaried compared to the initial values, showing no loss of activity in a physiologically
516 relevant time frame of 6 h. In contrast, the MICs values of lactose linoleate were found to be higher
517 (>1024 µg/mL) compared to the initial value (1024 µg/mL), an index of antimicrobial activity
518 reduction.

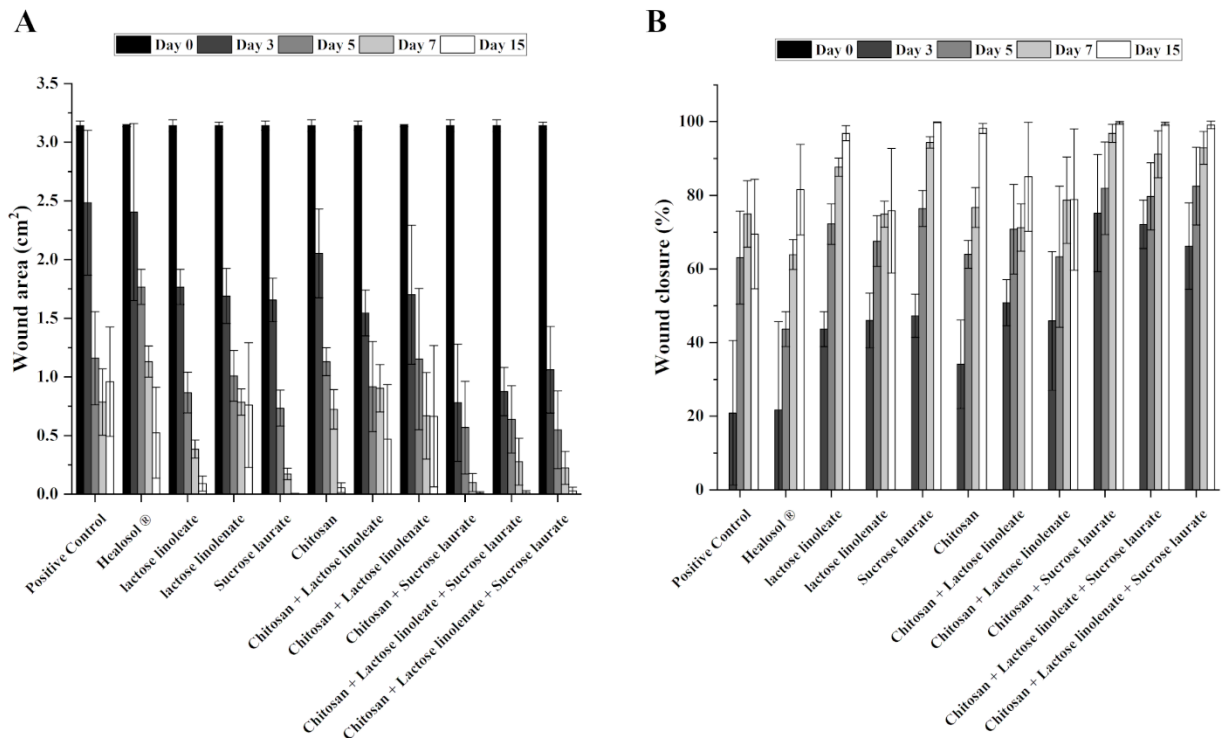
519
520 **3.7 *In vivo* studies**

521
522 **3.7.1 Sugar-based esters and their combinations with chitosan decreased the wound area and**
523 **accelerated wound closure.**

524 The gross appearances of the excision wounds in different groups were visualized at 3, 5, 7, and 15
525 days after injury (Supplementary material Figure 3). Obviously, on day 15, the untreated skin
526 wound (group II) naturally heal, however, there was still an unclosed wound. The healing process
527 was faster when the tested wound care solutions (*i.e.*, lactose linoleate, lactose linolenate, and
528 chitosan, both in single and mixed forms) were applied onto the wound, while a little imperfect
529 wound closure was also noticed yet at day 15 post-treatment. Strikingly, sucrose laurate solution
530 and its dual and triple mixtures displayed potentiated healing responses with almost the entire
531 closure of wounds at the end of the experiment.

532 According to the onset of healing response results, solutions of single components (*i.e.*, sucrose
533 laurate, lactose linoleate, and lactose linolenate) displayed a remarkable rapid onset of healing
534 response at 3 days after wounding (Figure 4). Their healing abilities were found to be significantly
535 faster than those that belonged to chitosan and the marketed product Healosol® as well as the
536 positive control of untreated wounds ($p < 0.05$). However, compared to solutions of single
537 components, dual and triple combinations showed a much more potent acceleration of wound
538 healing.

539 Notably, the time for 50% reduction of wound area was between 3 and 5 days, and 5 and 7 days
 540 after wound induction for solutions of tested single forms and marketed product were observed
 541 respectively (Figure 4A). Comparatively, more than 50% reduction in the wound area was achieved
 542 with rats treated with all dual and triple combinations at 3 days post-injury except chitosan and
 543 lactose linolenate combination that showed 50% wound contraction between 3 and 5 days (Figure
 544 4A).



545 **Figure 4.** Effects of sugar derivatives and their combinations on wound area and on percent of wound closure as a
 546 function of time in different treatment groups. Data are presented as mean \pm SEM (n = 6). (A) Wound area, (B) Wound
 547 closure.
 548
 549

550 It is worth mentioning that the wound closure in treated groups receiving chitosan, lactose linoleate,
 551 lactose linolenate solutions, and their combinations was lower than sucrose laurate treated groups.
 552 The lowest efficiency and incompletely healed tissue injuries were noticed with the rats treated with
 553 lactose linolenate, binary mixture of lactose linolenate and chitosan, and marketed product
 554 Healosal® showing only 78.84%, 84.79%, and 83.32% wound closure at the end of the treatment
 555 protocol (Figure 4B). On the other hand, the treated group receiving sucrose laurate solution and its
 556 mixed forms showed considerable restorative power of more than 90% wound closure in 7 days and
 557 wound recovery in 15 days post-injury.

558 To conclude, considering the comparison between the parallel treatments, sucrose laurate and its
 559 mixed forms were found to have the best efficiency in wound care among all the tested wound care
 560 forms in terms of acceleration of the cascade of wound healing adapt recovery of tissue injury.
 561

562 **3.7.2 Sugar-based esters and their combinations with chitosan resolved histopathological**
563 **alterations induced by wound and increased collagen formation during wound healing**

564 Histological examination of wound stained with H&E (Figure 5 and supplementary material Figure
565 4) showed normal histological structures of different skin layers in the control group with normal
566 hair follicles and minimal inflammatory cells infiltrates and normal subcutaneous layer. On the
567 other hand, persistent wide gap in the wound covered occasionally with scab from necrotic tissue
568 depress with obvious loss and necrosis of underlying epidermal layer were recorded in the positive
569 control (untreated) group, in marketed product Healosol[®] treated groups, chitosan treated group, in
570 lactose linolenate treated groups and in the combination of chitosan with lactose linoleate treated
571 group. These wounds were also filled with newly formed granulation tissue with abundant
572 inflammatory cells infiltrates accompanied by fibroblastic proliferation, focal subepidermal
573 hemorrhagic patches as well as newly formed blood vessels. However, positive control (untreated)
574 group and marketed product Healosol[®] treated groups demonstrated minimal quantitative records of
575 mature collagen fibers in dermal layer as shown in masson's trichrome stained tissue sections of all
576 samples.

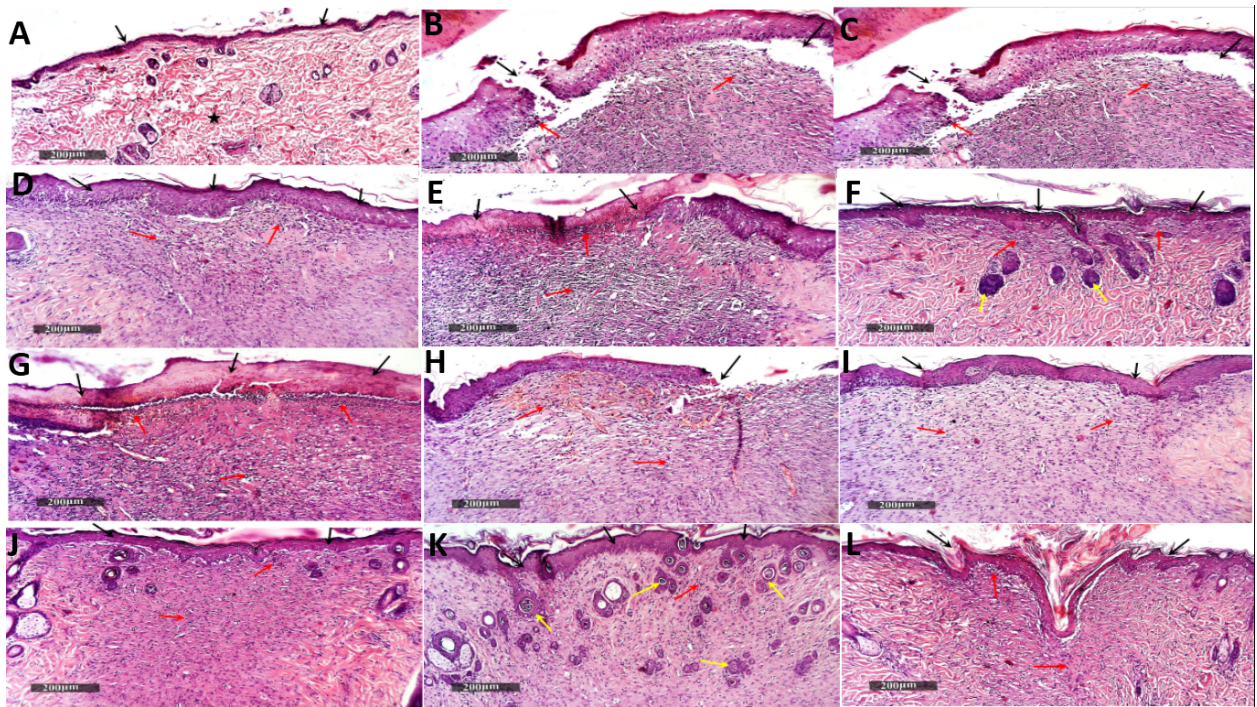
577 On the contrary, sucrose laurate or its combination with chitosan or the triple combination of
578 chitosan/sucrose laurate/lactose linoleate treated groups showed more accelerated wound healing
579 process with complete epidermal re-epithelialization and minimal persistence of subepidermal
580 granulation tissue with few inflammatory cells infiltrates as well as higher records of mature dermal
581 collagen fibers formation as shown in Masson's trichrome stained sections.

582 Similarly, lactose linoleate showed a more accelerated wound healing process with a wide wound
583 gap filled with granulation tissue with abundant fibroblastic activity and few inflammatory cells
584 infiltrates. Associated with complete epidermal re-epithelialization. However, lower records of
585 mature dermal collagen fibers formation were shown in Masson's trichrome stained sections
586 (Figure 6 and supplementary material Figure 5).

587 Interestingly, our results showed that the sucrose laurate treated group and its combination with
588 chitosan treated groups showed more accelerated new hair follicles formation.

589 Triple combination of chitosan/sucrose laurate/lactose linoleate showed complete epidermal re-
590 epithelialization and minimal persistence of subepidermal granulation tissue with minimal
591 inflammatory cells infiltrates. However, less accelerated records of mature dermal collagen fibers
592 formation were shown in Masson's trichrome stained sections (Figure 7). Moreover, more abundant
593 records of newly regenerated hair follicles were recorded (Supplementary material Table 9).

594



595
596

597 **Figure 5.** Effects of sugar derivatives and their combinations on histological alteration induced by wound:
598 photomicrographs of H&E stained sections of wound (scale bars 200 µm) (n=6) depicting:

599 (A) Control group shows demonstrated normal histological structures of different skin layers including apparent intact
600 epidermal layer with intact covering epithelium (arrow), intact dermal layer with normally distributed collagen fibers
601 (star), hair follicles and minimal inflammatory cells infiltrates, and normal subcutaneous layer were recorded.

602 (B) Positive control (untreated wound) group shows the persistence of wide area of wound gab covered occasionally
603 with scab from necrotic tissue depress with obvious loss and necrosis of underlying epidermal layer (arrow) and filled
604 with newly formed granulation tissue with abundant inflammatory cells infiltrates (red arrow), fibroblastic proliferation,
605 focal subepidermal hemorrhagic patches as well as newly formed blood vessels.

606 (C) Healosol[®] treated group shows the persistence of wide area of wound gab covered occasionally with scab from
607 necrotic tissue depress with obvious loss, necrosis of underlying epidermal layer with focal separation (arrow) with
608 abundant granulation tissue rich with inflammatory cells infiltrates (red arrow), fibroblastic proliferation, focal
609 subepidermal hemorrhagic patches as well as newly formed blood vessels.

610 (D) Lactose linoleate treated group shows accelerated wound healing process with complete epidermal re-
611 epithelialization (arrow) and minimal persistence of subepidermal granulation tissue with few inflammatory cells
612 infiltrates (red arrow).

613 (E) Lactose linolenate treated group shows persistence of wide area of wound gab covered occasionally with scab from
614 necrotic tissue depress with obvious loss and necrosis of underlying epidermal layer (arrow) and filled with newly
615 formed granulation tissue with abundant inflammatory cells infiltrates (red arrow), fibroblastic proliferation, focal
616 subepidermal hemorrhagic patches as well as newly formed blood vessels.

617 (F) Sucrose laurate treated group shows accelerated wound healing process were observed with complete epidermal re-
618 epithelialization (arrow) and minimal persistence of subepidermal granulation tissue with few inflammatory cells
619 infiltrates (red arrow). Moreover, newly regenerated hair follicles were shown (yellow arrow).

620 (G) Chitosan treated group shows persistence of a wide area of wound gab covered occasionally with scab from necrotic
621 tissue depress with obvious loss and necrosis of underlying epidermal layer (arrow) and filled with newly formed

622 granulation tissue with abundant inflammatory cells infiltrates (red arrow), fibroblastic proliferation, focal subepidermal
623 hemorrhagic patches as well as newly formed blood vessels.

624 (H) Chitosan/lactose linoleate treated group shows persistence of a wide area of wound gap covered occasionally with
625 scab from necrotic tissue depress with obvious loss, necrosis of underlying epidermal layer with focal separation
626 (arrow) with abundant granulation tissue rich with inflammatory cells infiltrates (red arrow), fibroblastic proliferation,
627 focal subepidermal hemorrhagic patches as well as newly formed blood vessels.

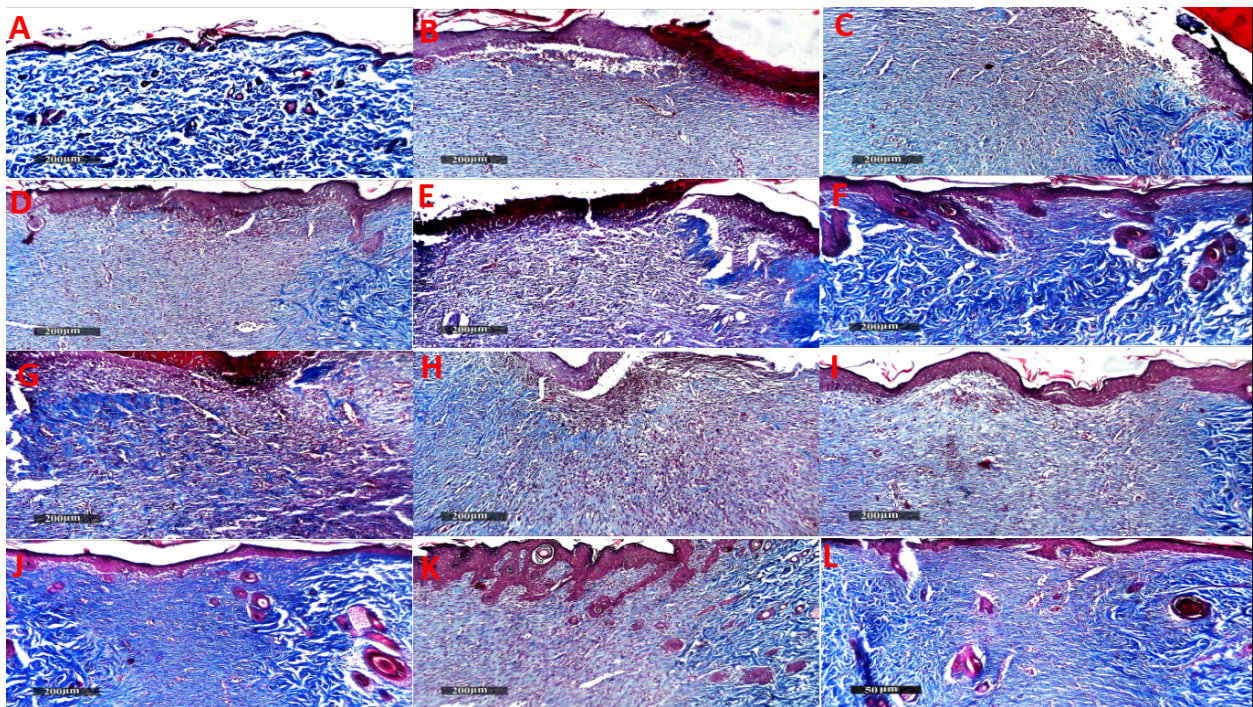
628 (I) Chitosan/lactose linolenate treated group shows more accelerated wound healing process with wide wound gap filled
629 with granulation tissue with abundant fibroblastic activity and few inflammatory cells infiltrates (red arrow), complete
630 epidermal re-epithelialization (arrow).

631 (J) Chitosan/sucrose laurate treated group shows accelerated wound healing process was observed with complete
632 epidermal re-epithelialization (arrow) and minimal persistence of subepidermal granulation tissue with few
633 inflammatory cells infiltrates (red arrow). Moreover, a higher rate of mature collagen fibers formation was recorded
634 with more accelerated new hair follicles formation (yellow arrow).

635 (K) Chitosan/lactose linoleate/sucrose laurate treated group shows complete epidermal re-epithelialization (arrow) and
636 minimal persistence of subepidermal granulation tissue with minimal inflammatory cells infiltrates (red arrow).
637 Moreover; more abundant records of newly regenerated hair follicles (yellow arrow) were shown.

638 (L) Chitosan/lactose linolenate/sucrose laurate treated group shows accelerated wound healing process was observed
639 with complete epidermal re-epithelialization (arrow) and minimal persistence of subepidermal granulation tissue with
640 few inflammatory cells infiltrates (red arrow).

641



642

643

644

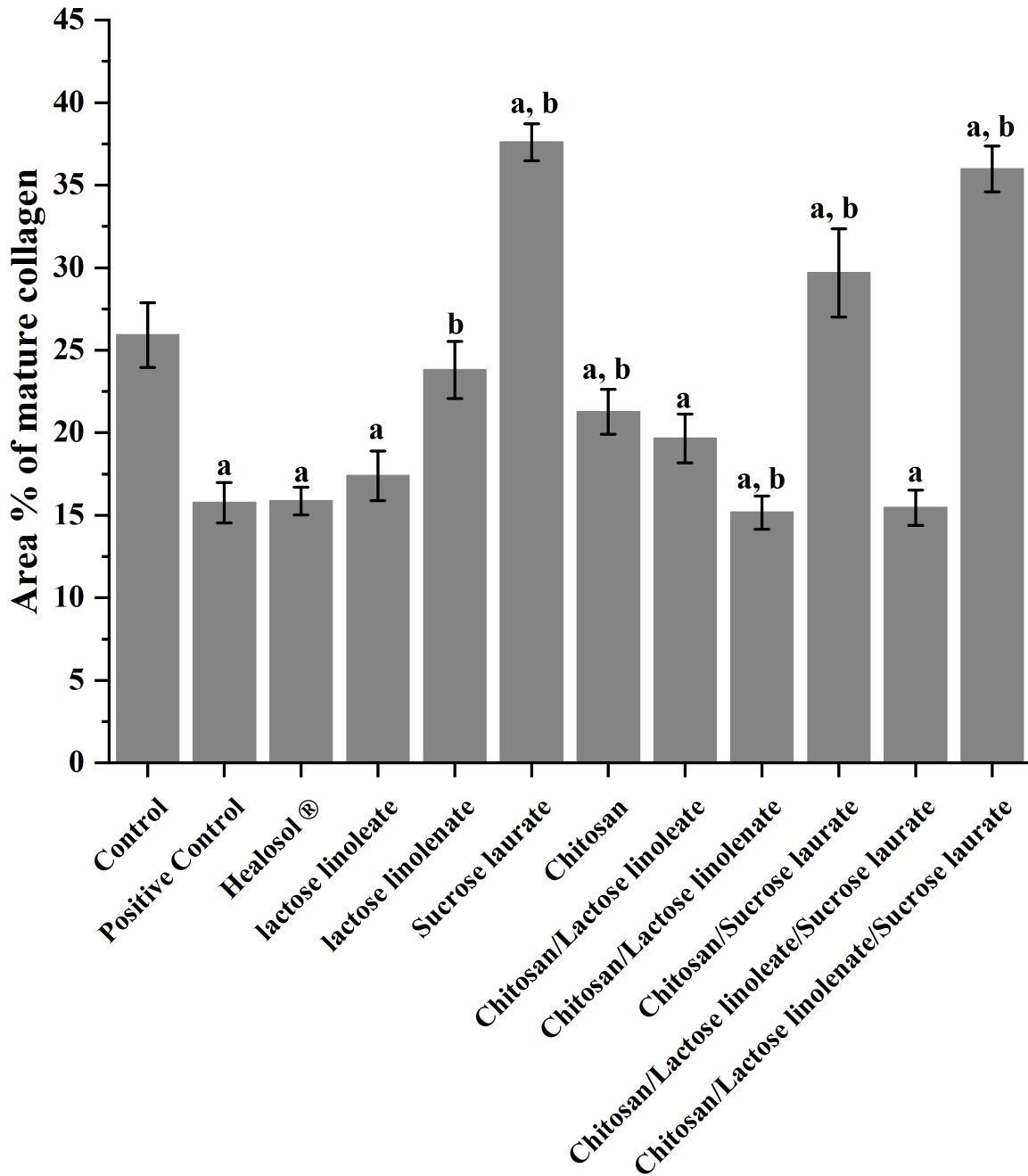
645

646

647

Figure 6. Effects of sugar derivatives and their combinations on collagen expression in different treatment groups: (A) Control group, (B) Positive control (untreated wound) group, (C) Healosol® treated group, (D) Lactose linoleate treated group, (E) Lactose linolenate treated group, (F) Sucrose laurate treated group, (G) Chitosan treated group, (H) Chitosan/lactose linoleate treated group, (I) Chitosan/lactose linolenate treated group, (J) Chitosan/sucrose

648 lauratreated group, (K) Chitosan/lactose linoleate/sucrose laurate treated group, (L) Chitosan/lactose
 649 linolenate/sucrose laurate treated group. (Scale bars 200µm) (n=6).
 650

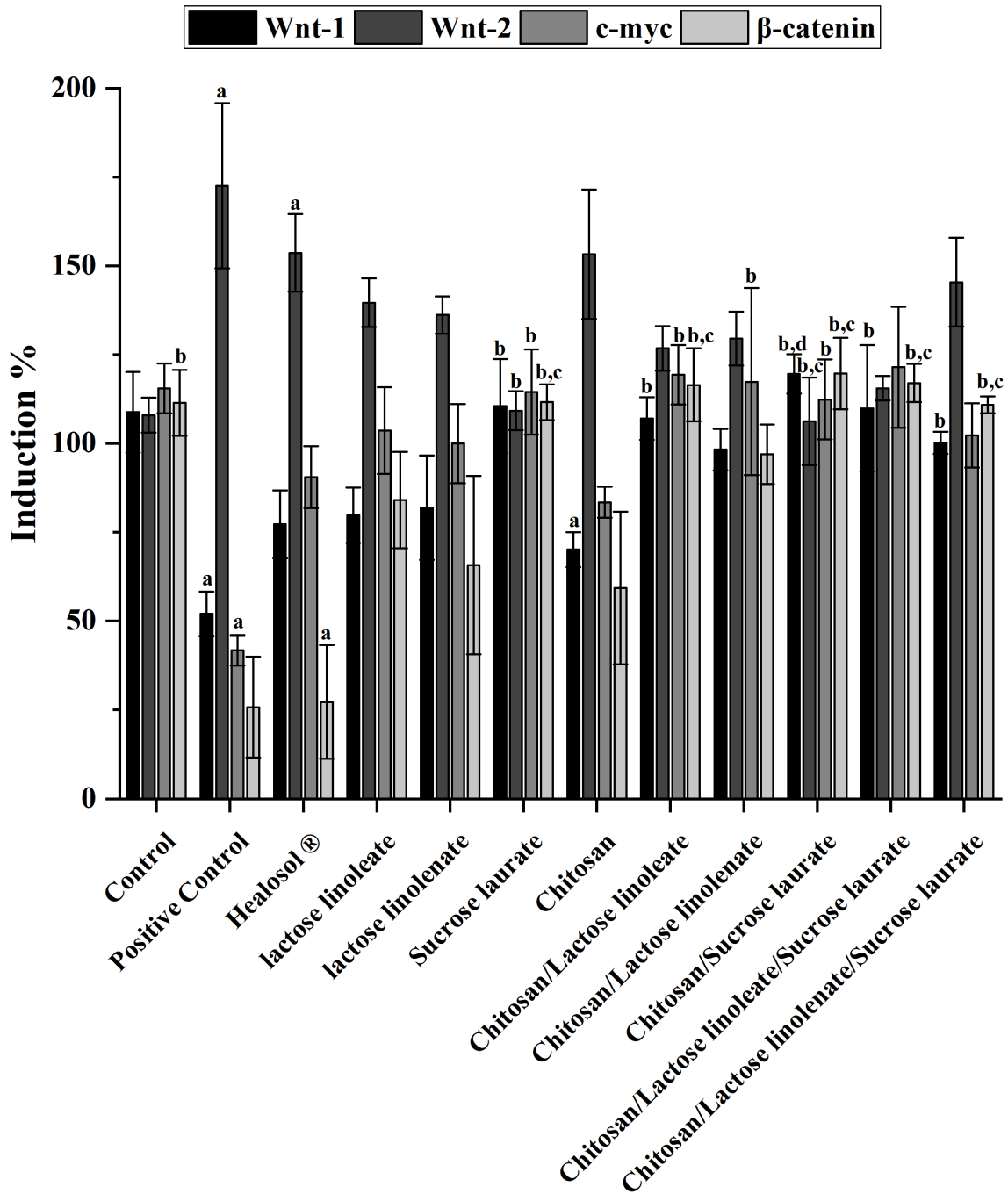


651
 652 **Figure 7.** Determination of area percentage of reactive collagen fibers to Masson's trichrome stain. Data are presented
 653 as mean ± SEM (n = 6). Statistical Analysis was performed using one-way ANOVA followed by Tukey's test as post-
 654 hoc test. a) Significantly different from Control group at p <0.05. b) Significantly different from Positive control group
 655 at p <0.05
 656

657 **3.7.3 Sugar-based esters and their combinations with chitosan restored disrupted Wnt/ β -**
658 **catenin signaling pathway during wound healing**

659 Knowing that the canonical Wnt/ β -catenin pathway is intricately involved in wound, inflammation
660 proliferation, remodeling regulation, and control of stem cells (Zhang et al., 2018), our study aimed
661 to investigate the effect of our biomaterials on the expression of key factors in Wnt/ β -catenin
662 signaling pathway. In fact, Wnt signaling is initiated by binding of Wnt ligands (as Wnt-1) to their
663 receptors, resulting in a cytoplasmic and nuclear increase of β -catenin which ultimately activates
664 target genes (as c-Myc) that function in many cellular processes (Shi et al., 2015). Whereas,
665 previous reports associated the important role played by c-myc in stimulating the epidermal stem
666 cells to accelerate wound healing (Waikel et al., 2001), thus its downregulation can induce delayed
667 wound healing (Frye et al., 2003). Furthermore, β -catenin was reported to be associated with
668 epidermal cell proliferation, differentiation, and migration (Zhang et al., 2012), and thus its increase
669 accelerates wound healing. Because Wnt-1 is a Wnt ligand, it was reported to activate the
670 β -catenin-dependent Wnt pathway (Kiesslich et al., 2010) and its increase was found to regulate
671 wound repair and regeneration of the skin (Lim and Nusse, 2013). On the other side, the Wnt-2
672 ligand was associated with skin fibrosis (Bayle et al., 2008). Whereas, its downregulation was
673 reported to block fibrosis in human keloid fibroblast (Cai et al., 2017).

674 Our results showed increased gene expressions of Wnt-1, c-myc and β -catenin in treated groups
675 receiving sucrose laurate and lactose linoleate both in single and combined formulations as
676 compared to the untreated wound group (positive control). However, groups treated with single
677 lactose linolenate showed a significant increase in c-myc gene expression with no significant
678 increase in Wnt-1 and β -catenin genes expression as compared to untreated wound group (positive
679 control). Alongside, no significant increase was detected in Wnt-1, c-myc and β -catenin genes
680 expression in chitosan or in marketed product Healosol[®] as compared to untreated wound group
681 (positive control). Meanwhile, chitosan showed significant decrease in Wnt-1 gene expression as
682 compared to unwounded group (negative control). Similarly, marketed product Healosol[®] showed
683 significant decrease in β -catenin gene expression as compared to unwounded group (negative
684 control), which highlights the superior beneficial effects of our biomaterials in either single or
685 combined formulations especially for sucrose laurate and lactose linoleate. Noteworthy, sucrose
686 laurate in single and combined formulations showed the highest increase in Wnt-1, c-myc, and β -
687 catenin genes expression. On the other side, a significant decrease in Wnt-2 gene expression was
688 reported in sucrose laurate single or combined formulations as compared to the untreated wound
689 group (positive control). Meanwhile, the marketed product Healosol[®] showed a significant increase
690 in Wnt-2 gene expression as compared to the unwounded group (negative control) (Figure 8).



692

693 **Figure 8.** Effects of sugar derivatives and their combinations on Wnt/ β -catenin signaling genes expression genes. Data
 694 are presented as mean \pm SEM (n = 6). statistical Analysis was performed using one-way ANOVA followed by Tukey's
 695 test as post-hoc test. a) Significantly different from Control group at $p < 0.05$; b) Significantly different from Positive
 696 control group at $p < 0.05$; c) Significantly different from Halosol® group at $p < 0.05$; d) Significant different from
 697 Chitosan group at $p < 0.05$.

698 **4. CONCLUSIONS**

699 The development and application of new biocompatible materials is a main challenge for
700 formulation scientists. Ideal wound dressing formulas must possess antioxidant, anti-inflammatory,
701 and antimicrobial properties and must induce skin regenerative activities. Here, we have been able
702 to synthesize and characterize new lactose-based sugar esters via a mild Steglich esterification.
703 Sucrose laurate, chitosan and the synthesized lactose linoleate and lactose linolenate were tested *in*
704 *vitro* and *in vivo* to evaluate their properties alone or as mixtures. They showed high
705 biocompatibility both *in vitro* and *in vivo*, coupled with antioxidant and anti-inflammatory effects,
706 accompanied by antimicrobial and antifungal activities. More specifically, the sugar esters (*i.e.*,
707 sucrose laurate and sucrose linoleate) and chitosan combinations showed a wound closure above
708 90% in male Wistar albino rats linked with the restoration of the Wnt/ β -catenin signaling. This
709 signaling modulates the inflammatory, and the oxidative stress states, and it controls stem cells to
710 induce epidermal cell proliferation which accelerates both wound healing and skin regeneration.
711 This innovative combination of biomaterials applied in wound dressing could effectively break new
712 ground in skin wound care.

713

714 **CRedit Authorship**

715 MT and EE: Investigation, data curation, formal analysis, methodology, visualization, and writing -
716 original draft;

717 MOE, SB, RC, MV, LP, FP, BC, MS, AD, SL: Formal analysis, investigation, methodology,
718 writing - review & editing;

719 MES, LC: Conceptualization, experimental design, supervision, data curation, writing - review &
720 editing and funding acquisition.

721

722 **Conflicts of interest**

723 The authors declare that they have no known competing financial interests or personal relationships
724 that could have appeared to influence the work reported in this paper.

725

726 **Funding**

727 This work was supported by Università di Urbino Carlo Bo, Urbino (PU), Italy (grant
728 DISB_CASSETTARI_ATENEO_SALUTE2018)

729

730 **5. REFERENCES**

731

732 Abd El-Hack, M.E., El-Saadony, M.T., Shafi, M.E., Zabermaawi, N.M., Arif, M., Batiha, G.E.,

733 Khafaga, A.F., Abd El-Hakim, Y.M., Al-Sagheer, A.A., 2020. Antimicrobial and antioxidant

734 properties of chitosan and its derivatives and their applications: A review. *Int. J. Biol.*

735 *Macromol.* 164, 2726–2744. <https://doi.org/10.1016/J.IJBIOMAC.2020.08.153>

736 Al-Sayed, E., Michel, H.E., Khattab, M.A., El-Shazly, M., Singab, A.N., 2020. Protective role of

737 casuarinin from melaleuca leucadendra against ethanol-induced gastric ulcer in rats. *Planta*

738 *Med.* 86, 32–44. <https://doi.org/10.1055/a-1031-7328>

739 Aldalaen, S., Nasr, M., El-Gogary, R.I., 2020. Angiogenesis and collagen promoting nutraceutical-

740 loaded nanovesicles for wound healing. *J. Drug Deliv. Sci. Technol.* 56, 101548.

741 <https://doi.org/10.1016/j.jddst.2020.101548>

742 Amini-Nik, S., Cambridge, E., Yu, W., Guo, A., Whetstone, H., Nadesan, P., Poon, R., Hinz, B.,

743 Alman, B.A., 2014. β -Catenin-regulated myeloid cell adhesion and migration determine

744 wound healing. *J. Clin. Invest.* 124, 2599–2610. <https://doi.org/10.1172/JCI62059>

745 Anstead, G.M., Hart, L.M., Sunahara, J.F., Liter, M.E., 1996. Phenytoin in wound healing. *Ann.*

746 *Pharmacother.* 30, 768–775. <https://doi.org/10.1177/106002809603000712>

747 Bayle, J., Fitch, J., Jacobsen, K., Kumar, R., Lafyatis, R., Lemaire, R., 2008. Increased expression

748 of Wnt2 and SFRP4 in Tsk mouse skin: Role of Wnt signaling in altered dermal fibrillin

749 deposition and systemic sclerosis. *J. Invest. Dermatol.* 128, 871–881.

750 <https://doi.org/10.1038/sj.jid.5701101>

751 Bryan, N.S., Grisham, M.B., 2007. Methods to detect nitric oxide and its metabolites in biological

752 samples. *Free Radic. Biol. Med.* 43, 645–647.

753 <https://doi.org/10.1016/j.freeradbiomed.2007.04.026>

754 Cai, Y., Zhu, S., Yang, W., Pan, M., Wang, C., Wu, W., 2017. Downregulation of β -catenin blocks

755 fibrosis via Wnt2 signaling in human keloid fibroblasts. *Tumor Biol.* 39, 1010428317707423.

756 <https://doi.org/10.1177/1010428317707423>

757 Campana, R., Merli, A., Verboni, M., Biondo, F., Favi, G., Duranti, A., Lucarini, S., 2019.

758 Synthesis and evaluation of saccharide-based aliphatic and aromatic esters as antimicrobial and

759 antibiofilm agents. *Pharmaceuticals* 12, 186. <https://doi.org/10.3390/ph12040186>

760 Catalani, S., Palma, F., Battistelli, S., Benedetti, S., 2017a. Oxidative stress and apoptosis induction

761 in human thyroid carcinoma cells exposed to the essential oil from *Pistacia lentiscus* aerial

762 parts. *PLoS One* 12, e0172138. <https://doi.org/10.1371/journal.pone.0172138>

763 Catalani, S., Palma, F., Battistelli, S., Nuvoli, B., Galati, R., Benedetti, S., 2017b. Reduced cell

764 viability and apoptosis induction in human thyroid carcinoma and mesothelioma cells exposed

765 to cidofovir. *Toxicol. Vitr.* 41, 49–55. <https://doi.org/10.1016/j.tiv.2017.02.008>

766 Chang, S.H., Lin, Y.Y., Wu, G.J., Huang, C.H., Tsai, G.J., 2019. Effect of chitosan molecular
767 weight on anti-inflammatory activity in the RAW 264.7 macrophage model. *Int. J. Biol.*
768 *Macromol.* 131, 167–175. <https://doi.org/10.1016/J.IJBIOMAC.2019.02.066>

769 Chongsiriwatana, N.P., Patch, J.A., Czyzewski, A.M., Dohm, M.T., Ivankin, A., Gidalevitz, D.,
770 Zuckermann, R.N., Barron, A.E., 2008. Peptoids that mimic the structure, function, and
771 mechanism of helical antimicrobial peptides. *Proc. Natl. Acad. Sci. U. S. A.* 105, 2794–2799.
772 <https://doi.org/10.1073/pnas.0708254105>

773 Elmowafy, E., El-derany, M.O., Biondo, F., Tiboni, M., Casettari, L., 2020. Quercetin Loaded
774 Monolaurate Sugar Esters-Based Niosomes: Sustained Release and Mutual Antioxidant –
775 Hepatoprotective Interplay, *Pharmaceutics* 12, 143.
776 <https://doi.org/10.3390/pharmaceutics12020143>

777 Farabegoli, F., Scarpa, E.S., Frati, A., Serafini, G., Papi, A., Spisni, E., Antonini, E., Benedetti, S.,
778 Ninfali, P., 2017. Betalains increase vitexin-2-O-xyloside cytotoxicity in CaCo-2 cancer cells.
779 *Food Chem.* 218, 356–364. <https://doi.org/10.1016/j.foodchem.2016.09.112>

780 Feng, P., Luo, Y., Ke, C., Qiu, H., Wang, W., Zhu, Y., Hou, R., Xu, L., Wu, S., 2021. Chitosan-
781 Based Functional Materials for Skin Wound Repair: Mechanisms and Applications. *Front.*
782 *Bioeng. Biotechnol.* 9, 650598. <https://doi.org/10.3389/fbioe.2021.650598>

783 Ferrer, M., Perez, G., Plou, F.J., Castell, J.V., Ballesteros, A., 2005. Antitumour activity of fatty
784 acid maltotriose esters obtained by enzymatic synthesis. *Biotechnol. Appl. Biochem.* 42, 35.
785 <https://doi.org/10.1042/ba20040122>

786 Frye, M., Gardner, C., Li, E.R., Arnold, I., Watt, F.M., 2003. Evidence that Myc activation depletes
787 the epidermal stem cell compartment by modulating adhesive interactions with the local
788 microenvironment. *Development.* <https://doi.org/10.1242/dev.00462>

789 Guan, Y., Chen, H., Zhong, Q., 2019. Nanoencapsulation of caffeic acid phenethyl ester in sucrose
790 fatty acid esters to improve activities against cancer cells. *J. Food Eng.* 246, 125–133.
791 <https://doi.org/10.1016/j.jfoodeng.2018.11.008>

792 Gumel, A.M., Annuar, M.S.M., Heidelberg, T., Chisti, Y., 2011. Lipase mediated synthesis of sugar
793 fatty acid esters. *Process Biochem.* 46, 2079–2090.
794 <https://doi.org/10.1016/j.procbio.2011.07.021>

795 Guth, F., Schiffter, H.A., Kolter, K., 2013. Novel excipients-from concept to launch. *Chim. Oggi-
796 Chem. Today* 31, 78–81.

797 Hough, L., Richardson, A.C., Thelwall, L.A.W., 1979. Reaction of lactose with 2,2-
798 dimethoxypropane: a tetraacetal of novel structure. *Carbohydrate Res.* 75, C11–C12.

799 [https://doi.org/10.1016/S0008-6215\(00\)84663-7](https://doi.org/10.1016/S0008-6215(00)84663-7)

800 Hu, H., Zhao, P., Liu, J., Ke, Q., Zhang, C., Guo, Y., Ding, H., 2018. Lanthanum
801 phosphate/chitosan scaffolds enhance cytocompatibility and osteogenic efficiency via the
802 Wnt/ β -catenin pathway. *J. Nanobiotechnol.* 16, 98. <https://doi.org/10.1186/s12951-018-0411-9>

803 Kale, S.S., Akamanchi, K.G., 2016. Trehalose Monooleate: A Potential Antiaggregation Agent for
804 Stabilization of Proteins. *Mol. Pharm.* 13, 4082–4093.
805 <https://doi.org/10.1021/acs.molpharmaceut.6b00686>

806 Khan, M.A., Mujahid, M., 2019. A review on recent advances in chitosan based composite for
807 hemostatic dressings. *Int. J. Biol. Macromol.* 124,138–147.
808 <https://doi.org/10.1016/j.ijbiomac.2018.11.045>

809 Kiesslich, T., Alinger, B., Wolkersdörfer, G.W., Ocker, M., Neureiter, D., Berr, F., 2010. Active
810 Wnt signalling is associated with low differentiation and high proliferation in human biliary
811 tract cancer in vitro and in vivo and is sensitive to pharmacological inhibition. *Int. J. Oncol.*
812 36, 49–58. https://doi.org/10.3892/ijo_00000474

813 Kim, S., Ng, W.K., Shen, S., Dong, Y., Tan, R.B.H., 2009. Phase behavior, microstructure
814 transition, and antiradical activity of sucrose laurate/propylene glycol/the essential oil of
815 *Melaleuca alternifolia*/water microemulsions. *Colloids Surfaces A Physicochem. Eng. Asp.*
816 348, 289–297. <https://doi.org/10.1016/J.COLSURFA.2009.07.043>

817 Klang, V., Novak, A., Wirth, M., Valenta, C., 2013. Semi-Solid o/w Emulsions Based on Sucrose
818 Stearates: Influence of Oil and Surfactant Type on Morphology and Rheological Properties. *J.*
819 *Dispers. Sci. Technol.* 34, 322–333. <https://doi.org/10.1080/01932691.2012.666187>

820 Krawczyk, J., 2018. Solid Wettability Modification via Adsorption of Antimicrobial Sucrose Fatty
821 Acid Esters and Some Other Sugar-Based Surfactants. *Mol.* 2018, 23, 1597.
822 <https://doi.org/10.3390/MOLECULES23071597>

823 Lamouille, S., Xu, J., Derynck, R., 2014. Molecular mechanisms of epithelial-mesenchymal
824 transition. *Nat. Rev. Mol. Cell Biol.* 15, 178–196. <https://doi.org/10.1038/nrm3758>

825 Lim, X., Nusse, R., 2013. Wnt signaling in skin development, homeostasis, and disease. *Cold*
826 *Spring Harb. Perspect. Biol.* 5, a008029. <https://doi.org/10.1101/cshperspect.a008029>

827 Lucarini, S., Fagioli, L., Campana, R., Cole, H., Duranti, A., Baffone, W., Vllasaliu, D., Casettari,
828 L., 2016. Unsaturated fatty acids lactose esters: cytotoxicity, permeability enhancement and
829 antimicrobial activity. *Eur. J. Pharm. Biopharm.* 107, 88–96.
830 <https://doi.org/10.1016/j.ejpb.2016.06.022>

831 Lucarini, S., Fagioli, L., Cavanagh, R., Liang, W., Perinelli, D.R., Campana, M., Stolnik, S., Lam,
832 J.K.W., Casettari, L., Duranti, A., 2018. Synthesis, structure–activity relationships and in vitro

833 toxicity profile of lactose-based fatty acid monoesters as possible drug permeability enhancers.
834 *Pharmaceutics* 10, 81. <https://doi.org/10.3390/pharmaceutics10030081>

835 Lukic, M., Pantelic, I., Savic, S., 2016. An overview of novel surfactants for formulation of
836 cosmetics with certain emphasis on acidic active substances. *Tenside, Surfactants, Deterg.* 53,
837 7–19. <https://doi.org/10.3139/113.110405>

838 Manzoor, M., Singh, J., Bandral, J.D., Gani, A., Shams, R., 2020. Food hydrocolloids: Functional,
839 nutraceutical and novel applications for delivery of bioactive compounds. *Int. J. Biol.*
840 *Macromol.* 165, 554–567. <https://doi.org/10.1016/j.ijbiomac.2020.09.182>

841 Marathe, S.J., Shah, N.N., Singhal, R.S., 2020. Enzymatic synthesis of fatty acid esters of trehalose:
842 Process optimization, characterization of the esters and evaluation of their bioactivities.
843 *Bioorg. Chem.* 94, 103460. <https://doi.org/10.1016/j.bioorg.2019.103460>

844 Mari, G., Catalani, S., Antonini, E., De Crescentini, L., Mantellini, F., Santeusanio, S., Lombardi,
845 P., Amicucci, A., Battistelli, S., Benedetti, S., Palma, F., 2018. Synthesis and biological
846 evaluation of novel heteroring-annulated pyrrolino-tetrahydroberberine analogues as
847 antioxidant agents. *Bioorg. Med. Chem.* 26, 5037–5044.
848 <https://doi.org/10.1016/j.bmc.2018.08.038>

849 Matica, M.A., Aachmann, F.L., Tøndervik, A., Sletta, H., Ostafe, V., 2019. Chitosan as a wound
850 dressing starting material: Antimicrobial properties and mode of action. *Int. J. Mol. Sci.*
851 <https://doi.org/10.3390/ijms20235889>

852 Matin, M., Roshid, M.H., Bhattacharjee, S., Azad, A., 2020. PASS Predication, Antiviral, in vitro
853 Antimicrobial, and ADMET Studies of Rhamnopyranoside Esters. *Med. Res. Arch.* 8.
854 <https://doi.org/10.18103/mra.v8i7.2165>

855 McCartney, F., Perinelli, D.R., Tiboni, M., Cavanagh, R., Lucarini, S., Filippo Palmieri, G.,
856 Casettari, L., Brayden, D.J., 2021. Permeability-enhancing effects of three laurate-disaccharide
857 monoesters across isolated rat intestinal mucosae. *Int. J. Pharm.* 601, 120593.
858 <https://doi.org/10.1016/j.ijpharm.2021.120593>

859 Mohan, K., Ganesan, A.R., Muralisankar, T., Jayakumar, R., Sathishkumar, P., Uthayakumar, V.,
860 Chandirasekar, R., Revathi, N., 2020. Recent insights into the extraction, characterization, and
861 bioactivities of chitin and chitosan from insects. *Trends Food Sci. Technol.* 105, 17–42.
862 <https://doi.org/10.1016/j.tifs.2020.08.016>

863 Neises, B., Steglich, W., 1978. Simple Method for the Esterification of Carboxylic Acids. *Angew.*
864 *Chemie Int. Ed. English* 17, 522–524. <https://doi.org/10.1002/anie.197805221>

865 Neta, N. do A.S., Santos, J.C.S. dos, Sancho, S. de O., Rodrigues, S., Gonçalves, L.R.B.,
866 Rodrigues, L.R., Teixeira, J.A., 2012. Enzymatic synthesis of sugar esters and their potential

867 as surface-active stabilizers of coconut milk emulsions. *Food Hydrocoll.* 27, 324–331.
868 <https://doi.org/10.1016/j.foodhyd.2011.10.009>

869 Neta, N.S., Teixeira, J.A., Rodrigues, L.R., 2015. Sugar Ester Surfactants: Enzymatic Synthesis and
870 Applications in Food Industry. *Crit. Rev. Food Sci. Nutr.* 55, 595–610.
871 <https://doi.org/10.1080/10408398.2012.667461>

872 Pérez, B., Anankanbil, S., Guo, Z., 2017. Synthesis of Sugar Fatty Acid Esters and Their Industrial
873 Utilizations, in: *Fatty Acids*. Elsevier, pp. 329–354. [https://doi.org/10.1016/b978-0-12-](https://doi.org/10.1016/b978-0-12-809521-8.00010-6)
874 [809521-8.00010-6](https://doi.org/10.1016/b978-0-12-809521-8.00010-6)

875 Perinelli, D.R., Lucarini, S., Fagioli, L., Campana, R., Vllasaliu, D., Duranti, A., Casettari, L., 2018.
876 Lactose oleate as new biocompatible surfactant for pharmaceutical applications. *Eur. J. Pharm.*
877 *Biopharm.* 124, 55–62. <https://doi.org/10.1016/j.ejpb.2017.12.008>

878 Saberian, M., Seyedjafari, E., Zargar, S.J., Mahdavi, F.S., Sanaei-rad, P., 2021. Fabrication and
879 characterization of alginate/chitosan hydrogel combined with honey and aloe vera for wound
880 dressing applications. *J. Appl. Polym. Sci.* 138, 1–15. <https://doi.org/10.1002/app.51398>

881 Saltarelli, R., Palma, F., Gioacchini, A.M., Calcabrini, C., Mancini, U., De Bellis, R., Stocchi, V.,
882 Potenza, L., 2019. Phytochemical composition, antioxidant and antiproliferative activities and
883 effects on nuclear DNA of ethanolic extract from an Italian mycelial isolate of *Ganoderma*
884 *lucidum*. *J. Ethnopharmacol.* 231, 464–473. <https://doi.org/10.1016/j.jep.2018.11.041>

885 Sanchez, M.C., Lancel, S., Boulanger, E., Nevriere, R., 2018. Targeting oxidative stress and
886 mitochondrial dysfunction in the treatment of impaired wound healing: A systematic review.
887 *Antioxidants.* 7, 98. <https://doi.org/10.3390/antiox7080098>

888 Schiefelbein, L., Keller, M., Weissmann, F., Lubber, M., Bracher, F., Frieß, W., 2010. Synthesis ,
889 characterization and assessment of suitability of trehalose fatty acid esters as alternatives for
890 polysorbates in protein formulation. *Eur. J. Pharm. Biopharm.* 76, 342–350.
891 <https://doi.org/10.1016/j.ejpb.2010.08.012>

892 Sferrazza, G., Corti, M., Brusotti, G., Pierimarchi, P., Temporini, C., Serafino, A., Calleri, E., 2020.
893 Nature-derived compounds modulating Wnt/ β -catenin pathway: a preventive and therapeutic
894 opportunity in neoplastic diseases. *Acta Pharm. Sin. B.* 10, 1814–1834.
895 <https://doi.org/10.1016/j.apsb.2019.12.019>

896 Shaw, J., Hughes, C.M., Lagan, K.M., Bell, P.M., 2007. The clinical effect of topical phenytoin on
897 wound healing: A systematic review. *Br. J. Dermatol.* 157, 997–1004.
898 <https://doi.org/10.1111/j.1365-2133.2007.08160.x>

899 Shi, Y., Shu, B., Yang, R., Xu, Y., Xing, B., Liu, J., Chen, L., Qi, S., Liu, X., Wang, P., Tang, J.,
900 Xie, J., 2015. Wnt and Notch signaling pathway involved in wound healing by targeting c-Myc

901 and Hes1 separately. *Stem Cell Res. Ther.* 6, 1–13. <https://doi.org/10.1186/s13287-015-0103-4>

902 Szuts, A., Láng, P., Ambrus, R., Kiss, L., Deli, M.A., Szabó-Révész, P., 2011. Applicability of
903 sucrose laurate as surfactant in solid dispersions prepared by melt technology. *Int. J. Pharm.*
904 410, 107–110. <https://doi.org/10.1016/j.ijpharm.2011.03.033>

905 Teng, Y., Stewart, S.G., Hai, Y.W., Li, X., Banwell, M.G., Lan, P., 2021. Sucrose fatty acid esters:
906 synthesis, emulsifying capacities, biological activities and structure-property profiles. *Crit.*
907 *Rev. Food Sci. Nutr.* 61, 3297–3317. <https://doi.org/10.1080/10408398.2020.1798346>

908 Tiboni, M., Coppari, S., Casettari, L., Guescini, M., Colomba, M., Fraternali, D., Gorassini, A.,
909 Verardo, G., Ramakrishna, S., Guidi, L., Di Giacomo, B., Mari, M., Molinaro, R., Albertini,
910 M.C., 2021. *Prunus spinosa* extract loaded in biomimetic nanoparticles evokes in vitro anti-
911 inflammatory and wound healing activities. *Nanomaterials* 11, 1–14.
912 <https://doi.org/10.3390/nano11010036>

913 Wagh, A., Shen, S., Shen, F.A., Miller, C.D., Walsha, M.K., 2012. Effect of lactose monolaurate on
914 pathogenic and nonpathogenic bacteria. *Appl. Environ. Microbiol.* 78, 3465–3468.
915 <https://doi.org/10.1128/AEM.07701-11>

916 Waikel, R.L., Kawachi, Y., Waikel, P.A., Wang, X.J., Roop, D.R., 2001. Deregulated expression of
917 c-Myc depletes epidermal stem cells. *Nat. Genet.* 28, 165–168. <https://doi.org/10.1038/88889>

918 Yang, H.L., Tsai, Y.C., Korivi, M., Chang, C.T., Hseu, Y.C., 2017. Lucidone Promotes the
919 Cutaneous Wound Healing Process via Activation of the PI3K/AKT, Wnt/ β -catenin and NF-
920 κ B Signaling Pathways. *Biochim. Biophys. Acta - Mol. Cell Res.* 1864, 151–168.
921 <https://doi.org/10.1016/j.bbamcr.2016.10.021>

922 Zhang, C., Chen, P., Fei, Y., Liu, B., Ma, K., Fu, X., Zhao, Z., Sun, T., Sheng, Z., 2012. Wnt/ β -
923 catenin signaling is critical for dedifferentiation of aged epidermal cells in vivo and in vitro.
924 *Aging Cell* 11, 14–23. <https://doi.org/10.1111/j.1474-9726.2011.00753.x>

925 Zhang, H., Nie, X., Shi, X., Zhao, J., Chen, Y., Yao, Q., Sun, C., Yang, J., 2018. Regulatory
926 mechanisms of the Wnt/ β -catenin pathway in diabetic cutaneous ulcers. *Front. Pharmacol.*
927 <https://doi.org/10.3389/fphar.2018.01114>

928 Zhang, X., Wei, W., Cao, X., Feng, F., 2015. Characterization of enzymatically prepared sugar
929 medium-chain fatty acid monoesters. *J. Sci. Food Agric.* 95, 1631–1637.
930 <https://doi.org/10.1002/jsfa.6863>

931 Zhao, L., Zhang, H., Hao, T., Li, S., 2015. In vitro antibacterial activities and mechanism of sugar
932 fatty acid esters against five food-related bacteria. *Food Chem.* 187, 370–377.
933 <https://doi.org/10.1016/j.foodchem.2015.04.108>

934 Zheng, Y., Zheng, M., Ma, Z., Xin, B., Guo, R., Xu, X., 2015. Sugar Fatty Acid Esters, in: *Polar*

935 Lipids: Biology, Chemistry, and Technology. Elsevier Inc., pp. 215–243.

936 <https://doi.org/10.1016/B978-1-63067-044-3.50012-1>

937